Oxytocin receptor controls promiscuity and development in prairie voles

Ruchira Sharma[1,2,3,4†], Kristen M. Berendzen[1,2,3,4†], Amanda Everitt[1,3,10,11], Belinda Wang[1,3], Gina Williams[1,2,3,4,5], Shuyu Wang[1,2,3,4], Kara Quine[1,2,3,4], Rose D. Larios[1,2,3,4,5,14], Kimberly L. P. Long[1,2,3,4], Nerissa Hoglen[1,2,3,4,5], Bibi Alika Sulaman[1,2,3,4,15], Marie C. Heath[1,2,3,4,16], Michael Sherman[1,2,3,4], Robert Klinkel[1,2,3,4,17], Angela Cai[1,2,3,4,20], Denis Galo[1,2,3,4,], Lizandro Chan Caamal[1,2,3,4,18], Nastacia L. Goodwin[1,2,3,4,19], Annaliese Beery[6,7], Karen L. Bales[8,9], Katherine S. Pollard[10,11,12], Arthur Jeremy Willsey[1,13], Devanand S. Manoli[1,2,3,4,*]

[1]Department of Psychiatry and Behavioral Sciences

[2]Center for Integrative Neuroscience

[3]Weill Institute for Neurosciences

[4]Kavli Institute for Fundamental Neuroscience

[5]Neurosciences Graduate Program, University of California, San Francisco; San Francisco, CA 95158, USA

[6]Department of Integrative Biology

[7]Department of Neuroscience, UC Berkeley, Berkeley, CA, United States

[8]Department of Psychology

[9]Department of Neurobiology, Physiology, and Behavior, University of California, Davis; Davis, CA 95616, USA

[10]Gladstone Institutes, San Francisco, CA, USA

[11]Department of Epidemiology & Biostatistics, University of California, San Francisco, San Francisco, CA, USA

[12]Chan Zuckerberg Biohub, San Francisco, CA, USA

[13]Calico Labs, San Francisco, CA 94080, USA

[14]Neurona Therapeutics, South San Francisco, CA 94080, USA

[15]Department of Neuroscience, University of Michigan, Ann Arbor, MI 48109, USA

[16]Department of Neurobiology and Behavior, University of California, Irvine; Irvine, CA 92697, USA

[17]Branch Out School, Los Angeles, CA 90026, USA

[18]University of California, Los Angeles; Los Angeles, CA 90095, USA

[19]Department of Psychology, University of Washington; Seattle, WA 98195, USA

[20]Department of Rehabilitation and Regenerative Medicine, Columbia University Irving Medical Center; New York, NY 10032, USA

* Corresponding authors. Devanand.manoli@ucsf.edu

Lead Contact: Devanand.manoli@ucsf.edu

†These authors contributed equally to this work

Summary:

Oxytocin receptor (Oxtr) signaling influences complex social behaviors in diverse species, including social monogamy in prairie voles. How Oxtr regulates specific components of social attachment behaviors and the neural mechanisms mediating them remains unknown. Here, we examine prairie voles lacking Oxtr and demonstrate that pair bonding comprises distinct behavioral modules: the preference for a bonded partner, and the rejection of novel potential mates. Our longitudinal study of social attachment shows that Oxtr sex-specifically influences early interactions between novel partners facilitating the formation of partner preference. Additionally, Oxtr suppresses promiscuity towards novel potential mates following pair bonding, contributing to rejection. Oxtr function regulates coordinated patterns of gene expression in regions implicated in attachment behaviors and regulates the expression of oxytocin in the paraventricular nucleus of the hypothalamus, a principal source of oxytocin. Thus, Oxtr controls genetically separable components of pair bonding behaviors and coordinates development of the neural substrates of attachment.

Keywords:

Attachment behaviors, prairie vole, pair-bonding, oxytocin receptor, partner preference, monogamy, promiscuity, oxytocin signaling, paraventricular nucleus of the hypothalamus, nucleus accumbens

Introduction

Social attachments, such as the bonds between parents and children, family and kin, friends, and the long-term relationships between mates and romantic partners form the basis of interpersonal and group dynamics within societies[1–7]. Various selective pressures have given rise to diverse patterns of complex social organization involving long-term relationships between members of a species, across mammals and other taxa, one of the most robust and intriguing of which is the enduring bond between mates[2,4,8–13]. In mammals, ~4% of species demonstrate social monogamy, forming persistent pair bonds between mating partners[9,14–16]. Comparative studies between closely related species that display distinct patterns of these social behaviors, including social monogamy, reveal correlated species-specific differences in the nonapeptide hormones oxytocin (Oxt) and arginine vasopressin (Avp), or their homologs, suggesting that they serve as critical modulators of affiliative behaviors and pair bonding[9–11,16–20]. Despite the central role of social attachment in human behavior and a rich history of investigation into the cognitive processes underlying social cognition and affiliative behaviors, it has been difficult to probe the neural mechanisms underlying these fascinating behaviors at the cellular, molecular, and genetic level, as most species that serve as model organisms for such studies in the laboratory do not display long-term social attachment as adults [6,21–27].

Prairie voles (*Microtus ochrogaster*) display long-term social attachment such that mating partners show an enduring pair bond and social monogamy[13,28–31]. Like many complex innate behaviors, pair bonding consists of distinct modules: the development of increased prosocial behaviors with partners over strangers (partner preference), and increased

agonistic behaviors towards novel opposite sex potential mates (stranger rejection)[13,30,32–37]. As in humans and other species that show affiliative social behaviors, disruption of pair bonds results in increased anxiety-like behaviors and markers of stress, supporting integrated neural and physiologic mechanisms that facilitate the preservation of such attachments[38–40]. Pioneering work in prairie voles identified Oxt and Avp as critical mediators of pair bonding[41,42]. Interspecific variations in the patterns of expression of the oxytocin receptor (Oxtr) and the vasopressin 1a receptor (V1ar) correlate with the potential for pair bonding within closely related vole species[43–49]. Consistently, pharmacologic inhibition of Oxt and Avp signaling via their respective cognate receptors disrupts pair bonding, while exogenous administration of these hormones promotes pair bonding without mating[28,50,51].

Given the central role of Oxt signaling in affiliative behaviors, we tested the genetic requirement for signaling via Oxtr for pair bonding and social behaviors in prairie voles. We generated prairie voles lacking Oxtr and unexpectedly observed that these animals continue to display a strong preference for partners following mating and cohabitation[52]. To gain deeper insight into the modulation of attachment and social behaviors by Oxtr function, we developed a series of behavioral assays to probe distinct aspects of pair bonding and associated social behaviors. To interrogate the molecular mechanisms mediating social attachment, we profiled patterns of gene expression in the nucleus accumbens (NAc), a key site of species differences associated with social monogamy that is dramatically enriched for Oxt binding in prairie voles[45,53,54]. We find that Oxtr controls the timing of pair bonding in prairie voles and promiscuity independent of partner

117 preference formation. Oxtr sex-specifically controls reciprocal social behaviors, such that
118 naïve wildtype (WT) males preferentially interact with wildtype females over those lacking
119 Oxtr, while wildtype females show no such bias towards WT males. Oxtr function
120 regulates patterns of gene expression in the NAc, as well as other regions of the vole
121 brain implicated in social and attachment behaviors, in distinct ways in each sex. Finally,
122 we find that Oxtr function regulates the development of Oxt and Avp expressing neurons
123 in the paraventricular nucleus, a principal source of these neuropeptides. Our studies
124 reveal genetically separable components of pair bonding and suggest that Oxtr signaling
125 sex-specifically participates in the development of the circuits underlying attachment
126 behaviors.

127 **Results**

128 **Oxtr function facilitates the formation of partner preference**

129 We previously found that Oxtr is not required for the display of partner preference
130 following 1 week of cohabitation[52]. However, acute modulation of Oxtr signaling can alter
131 patterns of social behaviors between individuals[29,50,55]. These observations suggest that
132 changes in Oxtr function may influence early social interactions that contribute to the
133 trajectory of pair bond formation and/or specific aspects of attachment behaviors following
134 the formation of partner preference. We first wished to determine whether Oxtr function
135 facilitated pair bond formation by examining the display of partner preference following
136 shorter periods of cohabitation. Consistent with previous studies showing that the
137 cohabitation time required for the display of partner preference differs between males and
138 females, we find that WT females demonstrate partner preference after only 6 hours of
139 cohousing with a WT male partner, while WT males require 5 days following introduction

140 to a potential WT mate (Fig. S1A-C)[56]. We therefore cohoused WT or Oxtr$^{1-/-}$ females with
141 WT males for 6 hours, and WT or Oxtr$^{1-/-}$ males with WT females for 5 days following
142 introduction (short cohabitation), or in these combinations for 1 or 7 days (long
143 cohabitation) for females or males, respectively (Fig. 1A, Fig. S1A).
144
145 Both males and females lacking Oxtr show an absence of partner preference following
146 short cohabitation with WT partners (Fig. 1B). Oxtr$^{1-/-}$ females, but not males, showed a
147 decrease in the fraction of huddling time with their partner and an increase in the fraction
148 of huddling time with a stranger compared to WT controls (Fig. 1C-D). Oxtr$^{1-/-}$ males
149 present an absence of partner preference (Fig. 1B), displayed due to both decreased time
150 with their cohoused partner and increased time with strangers (Fig. 1C-D). Consistent
151 with our previous studies, we find no difference between WT and Oxtr$^{1-/-}$ females when
152 the pairs are cohoused for the longer duration (Fig. S1B-F).
153
154 To further understand the dynamics of social interactions that contribute to the difference
155 in huddling behavior between WT animals vs their siblings lacking Oxtr following short
156 cohabitation, we quantified the cumulative time subjects spent huddling with their
157 cohoused partners or strangers over the course of the assay. Oxtr$^{1-/-}$ females show a
158 significant decrease in the amount of time spent huddling with partners in the last 30 mins
159 of the assay (150-180mins) (Fig. 1E). We also observe a significant increase in huddling
160 time of Oxtr$^{1-/-}$ males with strangers during the middle periods (75 – 130mins) (Fig. 1F),
161 suggesting that they engage in more early prosocial behavior with strangers than WT
162 males. Consistent with our previous work, we find no difference between cumulative

163 huddling times with either partner or stranger between WTs and Oxtr$^{1-/-}$ animals of both
164 sexes after long cohabitation periods (Fig. 1G-H)[45]. These observations demonstrate that
165 Oxtr function changes the temporal dynamics of social interactions with both familiar and
166 unfamiliar animal in a sex-specific manner. Taken together, our findings suggest that Oxtr
167 function acts early in the process of pair bonding to facilitate the formation of the partner
168 preference.
169

170 **Oxtr suppresses promiscuous behaviors in a state dependent manner in females**

171 Oxtr influences the dynamics of interactions with partners and strangers differently
172 between the sexes. We therefore wished to examine the detailed patterns of these
173 interactions separately in females and males (Fig. 2A). We examined the distribution of
174 huddles by WT vs Oxtr$^{1-/-}$ females following short cohabitation as a measure of prosocial
175 behavior displayed by these animals. We find that the top quartile of huddle durations
176 (long huddles) from each subject animal make up an average of ~90% of the total huddle
177 duration, functionally separating these interactions from incidental side-by-side contact
178 that may not constitute affiliative huddling (Fig. S2A Left). We classified long huddles as
179 partner huddles or stranger huddles and discovered that, consistent with the overall time
180 spent, the median huddle duration carried out by Oxtr$^{1-/-}$ females is significantly shorter
181 with partners and significantly longer with strangers, compared to WT females (Fig. 2B).
182 The longest huddle displayed with partner is significantly longer for WT females compared
183 to Oxtr$^{1-/-}$ females though we find no difference in the length of the overall longest huddle.
184 This is due to some Oxtr$^{1-/-}$ females conducting their longest huddle with the stranger
185 instead (Fig. S2B). Oxtr$^{1-/-}$ females additionally executed a larger number of huddles only

186 with the stranger, but not the partner, compared to WT controls (Fig. 2C). Taken together,
187 these results suggest that Oxtr function in females both facilitates prosocial behavior with
188 partners and suppresses such behavior with strangers during the early stages of pair
189 bond formation.
190
191 We next wished to determine whether the loss of Oxtr function influences patterns of
192 prosocial behaviors after the display of partner preference. We therefore examined
193 patterns of huddling, in particular the duration and frequency of these interactions,
194 following long cohabitation, a time point at which both WT and $Oxtr^{1-/-}$ animals display
195 robust preference for partners over strangers[52] (Fig. S1D). As with short cohabitation, the
196 top quartile of huddles (by duration) for each subject animal following long cohabitation,
197 described an average of 90% of total huddle time (Fig. S2A right). Following long
198 cohabitation, preference and huddling behavior in $Oxtr^{1-/-}$ females is indistinguishable
199 from their WT siblings (Fig. 2D-E). Comparing changes in the frequency of top quartile
200 huddles displayed by $Oxtr^{1-/-}$ females after short vs long cohabitation, we find that both
201 WT and $Oxtr^{1-/-}$ females show decreased huddle frequency with stranger following long
202 cohabitation (Fig. S2C-D). On comparing durations of long huddles, we find that $Oxtr^{1-/-}$
203 females significantly increase their median huddle duration with partner post long
204 cohousing (Fig. 2F-G). Thus, loss of Oxtr function in females reduces the duration of early
205 prosocial interactions (short cohabitation) with partners and strangers while Oxtr-
206 independent mechanisms eventually promote WT patterns of affiliative huddling and
207 partner preference following longer periods of cohabitation.
208

209 Our results suggest that Oxtr function influences specific aspects of early pair bonding
210 and attachment behaviors. We next wished to dissociate the influence of Oxtr on the
211 formation and display of partner preference from the display of agonistic rejection
212 behaviors towards novel strangers following cohabitation. We therefore developed a
213 battery of assays to examine initial social interactions between mating partners at early
214 and later stages of pair bonding, as well as stranger rejection following cohabitation
215 (Fig.2A). We examined the behavior of subject females from each genotype with WT
216 males when naive animals were first introduced to each other (Introduction), mating
217 behaviors following estrus induction (Timed Mating), prosocial interactions following
218 reunification with their bonded mate (Partner Reunification), and agonistic rejection of
219 novel, opposite sex strangers (Stranger Rejection) (Fig. 2A see Methods). We find no
220 differences in social behaviors during Introduction, Timed Mating and Partner
221 Reunification (Fig. 2H-J). In contrast, during Stranger Rejection, $Oxtr^{1-/-}$ females show
222 more social behaviors than WT females towards novel naive males in the absence of their
223 partner (Fig. 2K). Taken together, these studies demonstrate that Oxtr function regulates
224 specific components of pair bonding in females in a state-dependent manner, suppressing
225 promiscuous social interactions with stranger males after cohabitation sufficient for the
226 display of partner preference.
227

228 **Oxtr function influences different prosocial behaviors across the stages of pair**
229 **bonding in males**

230 Given the Oxtr-dependent difference in huddling behavior between males and females
231 after short cohabitation (Fig. 1C-D), we wished to assess sex differences in the patterns

232 of behaviors displayed by Oxtr$^{1-/-}$ animals and to further investigate Oxtr function in males
233 (Fig. 3A). Examining long huddles (as above, Fig. 2), we find that such huddles by Oxtr^{1-}
234 $^{/-}$ males with their partners following short cohabitation are significantly shorter when
235 compared to WT siblings, contributing to diminished partner preference early in pair
236 bonding (Fig. 3B Left). Interestingly, while Oxtr$^{1-/-}$ males show no difference in the total
237 amount of time spent huddling with strangers when compared to WT siblings (Fig. 1D),
238 they display shorter and more frequent huddles towards them at this time (Fig. 3B, 3C
239 Right). In males, Oxtr thus influences the pattern as well as amount of early affiliative
240 behavior to distinct behavioral stimuli in different ways.
241
242 Oxtr$^{1-/-}$ males show no difference in time spent with either partners or strangers after long
243 cohabitation (Fig. S1E-F). However, these males show a persistent reduction in the
244 duration of their long huddles with strangers at this time point (Fig. 3D). Following long
245 cohabitation, WT and Oxtr$^{1-/-}$ males show no difference in the duration of long huddles
246 with partners and a reduction in the duration of long huddles with strangers (Fig. S3A-B).
247 We find no difference in the frequency of long huddles between Oxtr$^{1-/-}$ and WT males
248 after long cohabitation (Fig. 3E). Consistently, comparing Oxtr$^{1-/-}$ males' behavior following
249 short vs long cohabitation reveals that the frequency with which Oxtr$^{1-/-}$ males huddle with
250 strangers decreases following long cohabitation (Fig. 3F-G). Thus, specifically in males,
251 loss of Oxtr function does not change the overall time spent huddling with strangers after
252 short or long cohabitation but does cause a continuing disruption in the patterns of
253 affiliative behavior that comprises huddling with strangers.
254

255 Our observations suggest that the loss of Oxtr disrupts certain characteristics of prosocial
256 behaviors in males regardless of the time spent bonding with their partner. We next
257 wished to dissect whether such loss of function resulted in atypical affiliative or agonistic
258 behaviors across stages of bonding. We examined the behavior of $Oxtr^{1-/-}$ males and their
259 WT siblings in the same series of paradigms described previously to characterize the
260 formation and maintenance of their pair bonds (Fig. 3A). $Oxtr^{1-/-}$ males spend similar
261 amounts of time as WT males engaging in prosocial behaviors with partners regardless
262 of bonding state (Fig. 3H-J, S3E). Similar to our observations in $Oxtr^{1-/-}$ females, $Oxtr^{1-/-}$
263 males spend more time engaging in prosocial behaviors with strangers in the absence of
264 their partners (Fig. 3K).
265
266 In contrast to time spent conducting mating behaviors with WT female partners (Fig. S3E),
267 $Oxtr^{1-/-}$ males demonstrate increased frequency of mating attempts when these females
268 are in estrus (Fig. 3I). Examining all instances of mounting, we find that $Oxtr^{1-/-}$ males
269 carry out shorter mounting bouts more frequently than WT males (Fig. S3F). To determine
270 whether the shorter bouts of mounting in $Oxtr^{1-/-}$ males influence the receptivity of their
271 partners, we compared the mount-to-intromission ratio for each animal[57] and find that
272 females are equally receptive to $Oxtr^{1-/-}$ males as their WT siblings (Fig. S3G). Thus,
273 consistent with our previous observations, Oxtr influences patterns, but not the amount
274 or success, of male mating behaviors, suggesting that such changes in males' behaviors
275 are equally able to elicit receptivity in females.
276

277 Compared to their WT siblings, naïve Oxtr$^{1-/-}$ males show decreased agonistic behaviors
278 towards an unfamiliar WT female upon first encountering her but display similar levels of
279 rejection of novel (unfamiliar) strangers upon bonding (Fig. S3C-D). Thus, Oxtr function
280 influences distinct components of males' attachment-related social behaviors towards
281 unfamiliar females at different points across pair-bonding, promoting agonistic displays
282 and lengthening mating bout durations when naïve, and suppressing promiscuous
283 prosocial behaviors upon bonding. Taken together our results suggest that Oxtr influences
284 patterns of social behaviors with future partners during the early phases of pair-bonding
285 differently in females and males, but upon bond formation, functions in both sexes to
286 suppress promiscuous affiliative behaviors towards strangers (Fig. S3H) without affecting
287 agonistic behaviors.
288

289 **Oxtr sex-specifically influences social interactions between potential mates**

290 Oxtr function influences patterns of social interactions between mates early during the
291 formation of a pair-bond (Short Cohabitation in both sexes, Introduction and Timed Mating
292 in males). We therefore investigated the effect of Oxtr loss on the choice made by a
293 potential mate. We developed a variation of the PPT three-chamber assay to present a
294 naive WT "chooser" with a choice between a naive opposite sex WT or naive opposite
295 sex Oxtr$^{1-/-}$ animal (Fig. 4A, Fig. S4A, see Methods). Strikingly, we find that Oxtr influences
296 the choice by a WT mate in a sex-specific manner. WT females choose WT or Oxtr$^{1-/-}$
297 males with equal frequency (Fig. 4B). In contrast, WT male choosers show significant
298 preference for WT females compared to Oxtr$^{1-/-}$ females, particularly during the middle of
299 the assay (150-280 mins) (Fig. 4B-C, Fig. S4B). These observations suggest that

300 disruption of Oxtr function specifically in females may alter their behavior such that WT
301 males prefer WT future partners over such mutants.
302
303 While naïve WT females show no difference in overall social choice between naive WT
304 and Oxtr$^{1-/-}$ males (WT-Oxtr$^{1-/-}$, Fig. 4B), they may show distinct behavioral dynamics in
305 the presence of an Oxtr$^{1-/-}$ male. To assess this, we compared the WT-Oxtr$^{1-/-}$ condition
306 with a control group in which the naive female chooser is given access to two naive WT
307 males (WT-WT) (Fig. 4D). We designated the tethered animal with whom the subject
308 spent More of Assay Time ("chosen") as the MOAT. Intriguingly, we found that the
309 presence of an Oxtr$^{1-/-}$ male (WT-Oxtr$^{1-/-}$) influenced the behavior of the WT female
310 chooser, such that they spent significantly more time with WT or Oxtr$^{1-/-}$ MOAT males
311 compared to the time spent with WT MOAT males from the WT-WT condition (Fig. 4E).
312 Consistent with this finding, naive WT female choosers break contact more frequently in
313 WT-WT conditions when compared to WT-Oxtr$^{1-/-}$ (Fig. 4F). Similarly, the divergence in
314 the amount of cumulative time spent with the MOAT for WT female choosers occurs after
315 5 hours have elapsed (320-360 mins) suggesting that complex interactions with males
316 lacking Oxtr influence how females "choose" a male partner regardless of whether they
317 end up choosing a WT or Oxtr$^{1-/-}$ MOAT (Fig. 4G). In contrast, we find no difference in the
318 contact time or number of such transitions when comparing naive WT male choosers with
319 MOAT females of a WT-WT vs WT-Oxtr$^{1-/-}$ condition (Fig. 4E-F).
320
321 We next examined the pattern of a WT chooser's interactions with both chosen (MOAT)
322 and unchosen animals (Less of Assay Time, LOAT) over time using a sliding preference

323 index (see Methods). We observed periods of convergence when choosers from a
324 condition (WT-WT or WT-Oxtr$^{1-/-}$) displayed significantly concurrent interactions with their
325 MOAT, indicated by the black bar above the trace. WT female choosers show a longer
326 and more consistent preference for their MOAT (regardless of genotype) in WT-Oxtr$^{1-/-}$ vs
327 WT-WT conditions, whereas WT male choosers show an earlier onset but equivalent
328 length of preference for MOATs in the WT-Oxtr$^{1-/-}$ condition compared with the WT-WT
329 condition (Fig. 4H). These observations suggest that interactions with males lacking Oxtr
330 influence the behavior of the WT females making a social choice, even when these
331 females interact more with and eventually choose a WT male. Taken together, loss of Oxtr
332 leads to differences in prosocial behaviors during initial interactions with WT naive
333 animals of the opposite sex that may later impact aspects of pair bonding.
334
335 Finally, to determine if naive prairie voles lacking Oxtr display generalized changes to
336 their behaviors independent of attachment-associated social behavior, we examined
337 general pro-social, anxiety-related, and locomotor behaviors. With the exception of an
338 increase in locomotion displayed by Oxtr$^{1-/-}$ females when compared to WT females in
339 an open field paradigm, we found no differences between Oxtr$^{1-/-}$ and WT voles of either
340 sex (Fig. S4C).
341
342 We have examined social interactions during the initial contact between mates, the
343 early stages of pair bonding, and during social attachment behaviors following partner
344 preference formation. Consistent with our findings and previous work, Oxtr function is
345 not required for the eventual display of partner preference. Here, we demonstrate that

346 Oxtr function sex-specifically facilitates early social interactions that contribute to the
347 formation of partner preference, and controls promiscuity.
348

349 **Oxtr controls the molecular signature of pair bonding in the nucleus accumbens**

350 We previously observed that Oxtr function is not required for the formation of partner
351 preference and here demonstrate that it suppresses prosocial behaviors towards novel
352 strangers following pair bonding. These results suggest that distinct components of pair
353 bonding are differentially influenced by Oxtr function or compensated upon its loss. We
354 next characterized the molecular signature associated with pair bonding to determine
355 whether changes in gene expression following pair bond formation are controlled by Oxtr.
356 Comparative studies demonstrate that Oxt binding in multiple brain regions differs
357 significantly between promiscuous and monogamous rodent species. Oxt binding is
358 particularly enriched in the NAc in prairie voles, while vasopressin binding is largely
359 absent in this area[45,47]. Thus, analyzing gene expression in the NAc allows us to identify
360 bonding-related expression that is primarily due to Oxtr function and largely independent
361 of the direct consequences of AVP signaling. Additionally, given the well-established role
362 of the NAc in the association of reward or aversion with specific sensory and
363 environmental cues[58–60] this region is well poised to play a role in the development of
364 partner preference, even without Oxtr signaling, as well as stranger rejection, which
365 appears to be dependent upon Oxtr function.
366

367 We performed bulk RNA-sequencing on NAc tissue from WT and $Oxtr^{1-/-}$ animals of both
368 sexes that were either: group housed with same-sex peers and sexually naïve (pre-

369 pairing); or paired with WT opposite-sex partners for six days, using our timed mating
370 paradigm (post-pairing) (Fig. 5A). PCA showed robust separation of WT and Oxtr$^{1-/-}$
371 samples (Fig. S5A). Differential expression (DE) analysis of pairing condition, regardless
372 of genotype or sex, identified 13 genes that show significant changes in expression post-
373 pairing (Fig. S5B), all of which showed decreased expression (Fig. 5B). These genes
374 include *Agt, Sgk1, Ptgds, Fosb, Pdk4*, and *Acsm5* (Fig. 5C) and, while these genes have
375 not previously been linked to shared gene regulatory or functional pathways, the predicted
376 protein-protein interaction network for the 13 DE genes shows more connections than
377 would be expected by chance ($p=2.47\ e^{-05}$) (Fig. S5C). Intriguingly, even in the limited set
378 of genes with altered expression in the context of pair bonding, changes are driven
379 primarily by expression in WT females (Fig. 5C, S5D). Subgroup analyses by genetic
380 background and sex identified additional genes including *Adora2a, Fkbp5*, and *Spred3* in
381 WT females and collagen-related genes, including *Col4a1* and *Col4a2*, in Oxtr$^{1-/-}$ females
382 (Fig. 5D, S5D). Only one gene, *Sema3b,* is significantly different in Oxtr$^{1-/-}$ males following
383 pairing (Fig. 5D).
384
385 To further examine changes in patterns of gene expression in the NAc associated with
386 pair bonding, we performed weighted gene coexpression network analysis (WGCNA)[61]
387 and calculated three sets of modules (M) from different sample subsets (modules^{WT} ,
388 modules^{Mut}, and modules^{All}) (Fig. S5F, S6D). Using the modules^{WT} subset, we identified
389 15 coexpression modules (Fig. S5F, Table 2) representing genes that share highly similar
390 expression patterns within the NAc. We identified one module (Mpink^{WT}) that significantly
391 and specifically correlated with pre-pairing status in WT animals (Pearson R correlation

392 of 0.7, Bonferroni adjusted p-value (p_{adj})=0.018) (Fig. 5E, S5E-F). Genes with high
393 module membership for the Mpink^{WT} are also those with high gene significance for pairing
394 condition supporting the module's association with behavior condition (Fig. 5SG). Further,
395 genes significantly differentially expressed with bonding are significantly enriched in
396 Mpink^{WT} (Bonferroni p_{adj}=7.44 e^{-08}) and serve as hub genes within this module (Fig. S5E,
397 G). These results suggest that the Mpink^{WT} module might be driving, or under the
398 influence of pathways driving, the pre-pairing to post-pairing state change.
399
400 We asked whether any of the modules^{WT} identified were regulated by Oxtr and thus lost
401 in Oxtr null animals. To address this, we assessed how well modules^{WT} are preserved in
402 mutant samples. We calculated a $Z_{summary}$ measure that combines module density and
403 intramodular connectivity metrics into a composite statistic. We find that of the modules^{WT},
404 Mpink^{WT} had the lowest $Z_{summary}$ ($Z_{summary}$ = 2) in Oxtr$^{1-/-}$ samples (Fig. 5F), indicating that
405 dynamics of gene expression that correlate with bonding states are lost in the absence of
406 Oxtr. Finally, the module eigengene (ME) for Mpink^{WT} when calculated for all 30 samples
407 and compared between pre- and post-pairing, was significant only for WT females
408 (Wilcoxon rank sum, Benjamini-Hochberg p_{adj}=0.03) and not for WT males or Oxtr$^{1-/-}$
409 animals of either sex (Fig. 5G). These observations suggest there is sex-specific,
410 coordinated regulation of gene expression in the NAc following pairing of mates that may
411 be associated with pair bond associated behaviors.
412

413 **Loss of Oxtr sex-specifically disrupts patterns of gene expression associated**
414 **with neurodevelopmental disorders**

415 We next wished to determine how Oxtr signaling contributes to changes in gene
416 expression in the NAc associated with the naive state or the process of pair bonding (Fig.
417 6A) by comparing the transcriptional profile of WT and $Oxtr^{1-/-}$ animals of each sex. We
418 observed significant genotype specific differences in gene expression in animals from
419 both sexes, with 466 genes showing differences between WT and $Oxtr^{1-/-}$ females, 270
420 between WT and $Oxtr^{1-/-}$ males, and 1,014 genes when samples from both sexes were
421 combined (using a $p_{adj}<0.05$ and absolute ($\log_2$(FC)) > 0.25 as criteria). Of the combined
422 DE gene set, 370 genes are upregulated and 644 are downregulated (Fig. 6B, S6A-B).
423 Genes with the greatest fold change across both sexes include *Slc2a3, Kcna1, Rgs8,*
424 *Cnksr2, Acvr*, and *Cnot6* (Fig. 6B). Genes specifically downregulated in $Oxtr^{1-/-}$ females
425 with $\log_2$(FC) less than 1 include *Abcb11* (a gene recently associated with treatment
426 resistant schizophrenia[62]), *Ngfr, Pon3,* and *Shh*. While there was no significant difference
427 in Oxtr transcript levels by genotype (p_{adj} = 0.753)—consistent with minimal nonsense-
428 mediated decay despite a premature stop codon—we have previously shown that no
429 functional protein is produced in $Oxtr^{1-/-}$ animals[52]. V1aR showed a modest decrease in
430 expression in $Oxtr^{1-/-}$ animals (p_{adj}=0.03) (Fig. S6C), though this is likely influenced by
431 variability in WT samples. WGCNA of all samples identified two modules ($Mbrown^{All}$ and
432 $Mturquoise^{All}$) that were significantly positively correlated with the WT genotype compared
433 to mutant (Pearson R = 0.55, p_{adj} = 0.011 for brown and Pearson R = 0.8, p_{adj} = 6.6e-7
434 for turquoise) (Fig. S6D). None of the identified modules showed correlation with pairing

435 condition (Fig. S6D). Our results thus reveal a dramatic change in patterns of gene
436 expression in the NAc with global loss of Oxtr signaling, independent of bonding state.
437
438 Examination of the sets of genes whose expression is altered by the loss of Oxtr,
439 regardless of bonding state or sex, revealed several distinct cellular processes regulated
440 by Oxtr signaling. These processes comprise larger domains of cell function including
441 extracellular channel binding activity, axoneme assembly complex, axon glial
442 ensheathment development, and metal cation transport (Fig. 6C), as well as pathways
443 for G protein signaling and dopaminergic neurogenesis (Fig. S6E). When analyzed by
444 sex, more of the identified processes were enriched in female Oxtr gene sets than in male
445 ones (female: 19/62, male: 6/62). To further link differentially expressed genes to
446 behavioral traits, we asked whether genes altered by loss of Oxtr are selectively enriched
447 for high-confidence associations with autism spectrum disorders (ASD) and other
448 neurodevelopmental diseases (NDD) affecting social attachment in humans as compared
449 to epilepsy, a disorder that does not disrupt social attachment[63–66]. Consistently, we find
450 that the genes upregulated with loss of Oxtr ($p_{adj}<0.01$, $\log_2(FC)>0$) are specifically
451 enriched for ASD- and NDD-associations but not epilepsy associations (Fig. 6D "Joint").
452 This enrichment is again primarily driven by genes upregulated in females and not males
453 (Fig. 6D). Thus, similar to the factors that influence gene expression changes associated
454 with pair bonding, many of the changes we identify in the NAc resulting from loss of Oxtr
455 are primarily driven by female-specific effects that may play a conserved role in mediating
456 social attachment in humans.
457

458 **Oxtr regulates coordinated gene expression across multiple neural populations**
459 **implicated in social attachment behaviors**

460 Given the expression of Oxtr in regions of the brain known to mediate social behavior in
461 voles and other species[67,68], we wished to determine if genes whose expression is altered
462 in the NAc by the loss of Oxtr were expressed not only in specific populations of cells
463 within this region, but in other regions of the prairie vole brain implicated in social and
464 attachment behaviors. We therefore examined the expression of 15 genes that showed
465 significant changes in expression in WT females when compared to those lacking Oxtr
466 using *in situ* hybridization (ISH) to both validate our RNA-seq findings as well as examine
467 the expression patterns of these genes. Several of these genes, such as
468 phosphodiesterase 10A (*Pde10A)* and diacylglycerol kinase beta (*Dgkb)*, show robust
469 expression throughout the striatum (data not shown), while genes such as the calcitonin
470 receptor (*Calcr*) and delta like non-canonical notch ligand 1 (*Dlk-1*) are expressed in
471 restricted populations of cells in the NAc (Fig. 6F-H, top panels). The expression of these
472 genes is significantly reduced in $Oxtr^{1-/-}$ females (Fig. 6E-H), supporting the specificity and
473 resolution of our RNA-seq findings.

474

475 In parallel to our examination of gene expression in the NAc, our ISH revealed that loss
476 of Oxtr in females altered the expression of the genes we examined in other regions of
477 the prairie vole brain. We examined the expression of these genes in the lateral septum
478 (LS), a region that has been implicated in agonistic and attachment behaviors in prairie
479 voles and other rodents and shows species dimorphic patterns of Oxt and Avp binding.
480 We observe that both *Calcr* and *Dlk-1* are decreased in the absence of Oxtr (Fig. 6G, H

481 middle panel) in the LS. We also find that expression of *Calcr* and *Dlk-1* is decreased in
482 the paraventricular nucleus of the hypothalamus (PVN), a principal source of Oxt and Avp
483 in the rodent brain which sends projections to the NAc (Fig. 6G-H bottom panels)[69–71].
484 These findings suggest that Oxtr function regulates patterns of gene expression in
485 multiple regions of the brain implicated in social and attachment behaviors in a
486 coordinated and region-specific manner.
487

488 **Loss of Oxtr results in the decrease in density of Oxt and Avp expressing**
489 **neurons in the PVN**

490 We find here that loss of Oxtr results in coordinated changes in gene expression in
491 multiple neural populations, including the PVN. We therefore wished to determine if the
492 signatures of gene expression regulated by Oxtr in the NAc in prairie voles (ONP set),
493 regardless of sex and bonding state, were enriched for patterns of gene expression
494 associated with distinct neural populations in other regions of the brain, particularly those
495 implicated in social and attachment behaviors. We compared the ONP gene set to the
496 molecular signatures of 33 hypothalamic subtypes previously identified by single-cell RNA
497 sequencing in mice[72]. Of the 33 clusters examined, the four with highest overlap with the
498 ONP gene set represent subsets of PVN neurons, in particular those that express Oxt
499 and AVP (Fig. 7A, clusters 43 and 26), as well as PVN neurons that express *Dlk1* and
500 *Calcr* (cluster 29), both of which show reduced expression in the NAc and PVN in females
501 lacking Oxtr (Fig. 6G-H bottom panel).
502

503 We next sought to determine if the overlap between Oxtr regulated genes and gene
504 expression patterns of neural populations in the PVN correlated with changes in the
505 expression of neuropeptides within PVN itself. We examined patterns of Oxt and Avp
506 expression using immunohistochemistry in naive adults and compared patterns of
507 expression between WT animals of both sexes and those lacking Oxtr (Fig. 7B, Fig.
508 S7A-B). We find that the density of both Oxt and Avp producing neurons is lower in
509 $Oxtr^{1-/-}$ animals (Fig. 7C-E). To determine if the loss of Oxt or Avp expression was
510 restricted to specific populations of PVN neurons, we examined the expression of these
511 peptides across the anterior-posterior axis of the PVN in both WT and $Oxtr^{1-/-}$ males and
512 females. We find that animals of both sexes show a preferential loss of Oxt and Avp
513 expressing neurons in the anterior PVN (Fig. 7F-G). Finally, we examined patterns of
514 Oxt and Avp over the course of development to determine when loss of Oxtr function
515 influences the development of their expression. We find that the density of Oxt neurons
516 at P0 (Fig. S7C-F) and both Oxt and Avp neurons at P21 is lower in $Oxtr^{1-/-}$ females
517 compared to age matched WT females (Fig. S7G-J). In contrast, we find that Oxt and
518 Avp neuron density loss occurs only in adult $Oxtr^{1-/-}$ males (Fig. 7D-G, Fig. S7B). These
519 observations suggest the coordinated, region-, and sex-specific influence of Oxtr
520 function on the development of neurons expressing Oxt (and Avp) within the PVN,
521 consistent with a trophic role for this pathway identified in mice[73–76].
522

523 **Discussion**

524 Robust reproductive behaviors are essential for survival. Accordingly, species have
525 evolved diverse strategies, including social monogamy, which mediate locating,

526 identifying, and attracting mates, facilitate reproduction, and promote the survival of
527 progeny[16,77]. Signaling via Oxtr influences a wide range of physiology and behavior
528 associated with social interactions and attachment between conspecifics, including pair
529 bonding between prairie vole mates[41,78]. Our recent findings that Oxtr is not genetically
530 required for the formation of partner preference in prairie voles suggests that, like other
531 genes and neuromodulatory pathways across diverse species, Oxtr likely functions in
532 parallel to multiple genetically specified pathways to facilitate pair bonding by influencing
533 specific behavioral modules that contribute to the complex behaviors that comprise social
534 attachment[33,35,79–85].
535
536 Here we demonstrate that loss of Oxtr in prairie voles influences the dynamics of social
537 interactions between sexually naïve animals and WT potential mates in distinct social
538 contexts in sex-specific ways. When given a choice, naive WT males display a preference
539 for WT females rather than for those lacking Oxtr, supporting the role of Oxtr in controlling
540 behavior during an early, sensitive period in bond formation[30]. The presence of an Oxtr^{1-}
541 $^{/-}$ male alters levels and patterns of early prosocial behavior exhibited by WT females,
542 without ultimately affecting their choice of potential partner. Taken together, these
543 observations suggest that Oxtr may modulate social behaviors that act early in a sensitive
544 pair bond formation period, and via these behaviors or yet-to-be-determined sensory cues
545 such as pheromone profiles or patterns of vocal communication, influences the reciprocal
546 behavior of partners.
547

548 Animals lacking Oxtr take longer to display partner preference, and despite strong partner
549 preference following longer cohabitation, demonstrate promiscuous prosocial behaviors
550 towards novel potential mates, including huddling with strangers. These observations are
551 consistent with a state-dependent role of Oxtr function, similar to findings in multiple
552 species, including humans[86–88]. Oxtr function may thus promote prosocial behavior in the
553 naïve state to facilitate attachment with an unfamiliar potential mate, but following pair
554 bond formation, suppresses further prosocial interactions to new individuals, or even
555 promotes further separation from and rejection of unfamiliar individuals or groups. Across
556 species and outside of the context of pair bonding, oxytocin signaling may play a
557 conserved role in mediating other state-specific aversive behavior, for example, defeat-
558 induced social avoidance learning[89].
559
560 Our findings reveal that patterns of social behaviors contributing to 1) pair bond formation,
561 2) partner preference, and 3) rejection of novel mates are genetically separable
562 components of pair bonding representing distinct behavioral modules regulated by
563 mechanisms that require Oxtr function, i.e. reciprocal behaviors and stranger rejection, or
564 those that can be displayed in its absence, i.e. partner preference. Further work will allow
565 us to determine the Oxtr-independent mechanisms that mediate the closure of an early
566 sensitive period and facilitate the display of partner preference[52]. Where Oxtr functions
567 to control the switch from prosocial behavior towards a potential mate in naïve animals to
568 the suppression of such behaviors towards, and active rejection of, opposite-sex
569 conspecific strangers following bonding remains to be determined.
570

571 Examination of the molecular signatures of pair bonding and the role of Oxtr in regulating
572 these changes in gene expression in the NAc reveals modest, Oxtr-dependent changes
573 in the expression of a specific network of genes in WT animals following pair bonding[45,90].
574 Intriguingly, loss of Oxtr preferentially impacts patterns of gene expression in the NAc in
575 females. The NAc demonstrates little endogenous sex steroid hormone receptor
576 expression difference in gene expression in prairie voles and other species[67,91–93]. Sex
577 differences in the effects of Oxtr on gene expression this region may therefore suggest
578 that there are significant sex-differences in the inputs into this region that act through Oxtr
579 during development[94–99]. The larger impact of loss of Oxtr in females is consistent with its
580 more general conservation in mammals to regulate aspects of female physiology such as
581 lactation and prosocial behaviors or sensory cues that promote interactions with males[100].
582
583 Genes with altered expression in the absence of Oxtr are enriched for genes associated
584 with neuropsychiatric disorders, in particular neurodevelopmental disorders and ASD.
585 Given the sex-biased enrichment of these genes, such developmental differences in the
586 impacts of Oxtr function may contribute to sex differences in the pathophysiology of these
587 disorders[101–103]. Accordingly, the molecular signatures of attachment in the NAc, both
588 dependent upon and independent of Oxtr function, are subtle relative to these sex-biased
589 differences in the role of Oxtr and possibly reside in other neural populations that function
590 in attachment.
591
592 Validation of changes in gene expression in the NAc resulting from loss of Oxtr suggests
593 coordinated regulation of these genes by Oxtr across multiple brain regions implicated in

594 social and attachment behaviors. Oxtr may be one of multiple factors that organizes
595 specific components of the circuits underlying these displays to control discreet modules
596 of behavior. Consistent with a trophic role for Oxtr function during development, we find
597 that the genes regulated by Oxtr within the NAc are enriched for those that identify cell
598 types in the PVN, a principal source of neuropeptides implicated in pair bonding, which
599 sends oxytocinergic projections to the NAc[68,70,104–106]. Loss of Oxtr preferentially impacts
600 Oxt and Avp expression in the anterior PVN, suggesting that specific populations of these
601 cells may be more dependent upon such trophic function for their development, survival,
602 or expression of these hormones. Whole brain analysis will likely reveal if such neurons
603 have distinct projections when compared to those that remain in the absence of Oxtr,
604 contributing to our understanding of how these circuits and pathways regulate distinct
605 aspects of social and attachment behaviors and physiology[4,78,107].
606
607 Taken together, our behavioral and molecular studies reveal previously unappreciated
608 nuances in the control of social behavior and pair bonding by Oxtr function. They uncover
609 intriguing sex differences in the patterns of behavior influenced by loss of Oxtr function.
610 These observations suggest that circuits with sex-specific patterns of development, or
611 even function in ancestral species, may mechanistically converge in the context of Oxtr
612 function to generate displays of reciprocal interactions, pair bonding and attachment
613 behaviors in WT prairie voles that are similar between males and females[108,109].
614 Manipulation of Oxtr expression at specific developmental timepoints and in specific
615 neural populations will help to elucidate how this pathway influences social and
616 attachment behaviors in the context of normal development to regulate distinct

617 components of pair bonding. Understanding the specific neural populations that express
618 Oxtr and other molecular pathways that contribute to pair bonding will allow us to
619 understand the mechanisms controlling the early experience-dependent, sensitive period
620 of bond formation. In parallel, examination of the activity in these populations following
621 manipulations of Oxtr function will allow us to determine the circuit mechanisms by which
622 similar but distinct sensory cues contribute to the identification of partners or novel
623 conspecifics and consequently, the display of dramatically different patterns of social
624 behaviors. The sum of these mechanisms represents the preference for partners over
625 strangers and reflects the formation and maintenance of pair bonds between mates,
626 affiliation between individuals, and the behavioral consequences of identifying others as
627 unfamiliar or outside of these bonds.
628

629 **Acknowledgments**

630 The authors would like to thank members of the Manoli lab for assistance, advice,
631 helpful discussion and comments on the manuscript. J. Tollkuhn and M. Brainard
632 provided valuable insights to the structure, content and design of the manuscript.
633 Additionally, we would like to thank S. Garg for his assistance in data analysis and help
634 designing the analytic pipeline. The authors received funding from National Institutes of
635 Health grant R01MH123513 (D.S.M.), National Science Foundation grant 1556974
636 (D.S.M.), Burroughs Wellcome Fund 1015667 (D.S.M.), Whitehall Foundation grant
637 2018-08-83 (D.S.M.), One Mind Foundation A137726 (D.S.M.), National Institutes of
638 Health grant R25MH060482 (K.M.B.), AP Giannini Foundation Fellowship P0534952

(K.M.B.), Larry L. Hillblom Foundation Fellowship 2020-A-023-FEL (K.M.B.), and National Institute of Mental Health grant R01MH123178 (K.S.P.)

Author contributions

Conceptualization, R.S., K.M.B., K.L., and D.S.M.; methodology, A.B., A.J.W., D.S.M., K.L.B., K.M.B., K.S.P., and R.S.; software, K.Q., and S.W.; formal analysis, A.E., R.S., and K.M.B.; investigation, R.S., K.M.B., A.E., B.W., G.W., S.W., K.Q., R.D.L., K.L., N.H., B.A.S., M.C.H., M.S., R.K., A.C., D.G., L.C.C., N.L.G.; visualization, R.S., K.M.B., B.W., and A.E.; funding acquisition, D.S.M., K.S.P., and A.J.W; writing– original draft, R.S., and K.M.B.; writing-review & editing, R.S., K.M.B., D.S.M., N.H., K.S.P., A.E., and A.B.

Declaration of interests

The authors declare no competing interests.

Star Methods

Key resources table

REAGENT or RESOURCE	SOURCE	IDENTIFIER
Chemicals, peptides, and recombinant proteins		
DAPI	Sigma-Aldrich	Cat #D9542; CAS #28718-90-3

Experimental models: Organisms/strains		
Prairie vole: OxtR$^{1-/-}$	Berendzen et al.	
Oligonucleotides		
ISH probes	This paper	N/A
Oxtr$^{1-/-}$ genotyping oligos	This paper	N/A
Antibodies		
Oxytocin Polyclonal	Invitrogen	Cat#PA5-26701; RRID
Anti-Neurophysin 2/NP-AVP	Millipore	Cat#MABN845; RRID
Cy™3 AffiniPure Donkey Anti-Rabbit IgG	Jackson ImmunoResearch	Cat #711-165-152; RRID
Alexa Flour 488 Donkey Anti Mouse IgG	Thermo Fisher Scientific	Cat #711-165-152; RRID
Software and algorithms		
ImageJ	NIH	; RRID: SCR_003070
R (version 1.1.423)	R Core	https://www.r-project.org/
GraphPad Prism (version 7.03)	GraphPad Software	
Boris	Boris	www.boris.unito.it

MATLAB	MathWorks	https://www.mathworks.com/products.html RRID: SCR_001622

654

655 **Resource availability**

656 **Lead contact**

657 Further information and requests for resources and reagents should be directed to and

658 will be fulfilled by the lead contact, Devanand Manoli (devanand.manoli@ucsf.edu).

659 **Materials availability**

660 All unique reagents generated in this study are available from the lead contact upon

661 request.

662 **Data**

663 Transcriptomics data discussed in this publication are accessible through GEO Series

664 accession number GSE279248.

665 **Code**

666 All code used for RNA-seq data processing and differential expression analyses, as well

667 as post-processed expression data, can be found at

668 https://github.com/aseveritt/OXTR_prairie_voles

669

670 **EXPERIMENTAL MODEL AND SUBJECT DETAILS**

671 **Animals**

672 Subjects were laboratory-bred prairie voles (*Microtus ochrogaster*) which originated
673 through systematic outbreeding of a wild stock captured near Champaign, Illinois.
674 CRISPR/Cas9 editing was used to generate 2 independent null alleles, $Oxtr^{1-/-}$ and
675 $Oxtr^{2-/-}$, both of which were validated using autoradiography to show loss of receptor
676 function[52] (data not shown). $Oxtr^{1-/-}$ was backcrossed for >7 generations to mitigate any
677 possible off-target effects and this line was used for all subsequent experiments.
678 Sexually naïve male and female animals were group weaned at 21 ± 1 days and
679 separated to group housing with same-sex siblings and age-matched same-sex non-
680 siblings. Voles were maintained under a 14:10 h light-dark cycle in clear plastic cages
681 (45 × 25 × 15 cm) with bedding, nesting material (nestlet), and a PVC hiding tube.
682 Rooms were maintained at approximately 20°C, and food and water were available *ad*
683 *libitum*.

684

685 Breeding pairs were established between two heterozygotes or a homozygous $Oxtr^{1-/-}$
686 mutant male and heterozygous female partner from a breeding line maintained in the
687 lab. Voles were randomly assigned into experimental groups when they reached 7-9
688 weeks of age at the start of testing. This study was carried out in accordance with the
689 recommendations in the Guide for the Care and Use of Laboratory Animals published
690 by the National Research Council. The protocol was approved by the Institutional
691 Animal Care and Use Committee at each respective institution.

692 **Genotyping**

693 The following primers were used to amplify a region where XcmI restriction for $Oxtr^1$ or
694 Bpu10I restriction for $Oxtr^2$ determined the genotype of all animals studied. XcmI cuts
695 the mutant allele in the case of $Oxtr^1$ and Bpu10I restricts the WT sequence for $Oxtr^2$.
696 (Forward: ACTGGAGCTTCGAGTTGGAC, Reverse: ATGCCCACCACTTGCAAGTA)

697 **METHOD DETAILS**

698 **Behavior**

699 ***Triadic naive choice assay***

700 The linear three chamber partner preference apparatus with open top and 10 x 32 inch
701 walls[52] was modified to capture the interactions of the naive, freely moving WT subject
702 and the naive, tethered, opposite sex potential partner (either 2 WTs or a WT and an
703 $Oxtr^{1-/-}$) at either end of the chamber. Behaviors were recorded for 6 hours using a top
704 view camera and the videos generated were analyzed using a contour detection
705 algorithm. Specifically, contours were detected on individual video frames using a
706 threshold-based strategy that took advantage of the contrast between dark-colored vole
707 fur coats and light-colored bedding and chamber apparatus. A standalone vole was
708 detected as a single contour, and two voles in physical contact were likewise detected
709 as a single contour. Consistent vole identities across video frames were determined
710 using the Hungarian algorithm. Since the assay began with one vole in each of the three
711 chambers, and since the subject vole remained freely mobile throughout, it was possible
712 to unambiguously assign each contour to a single vole identity (e.g., subject, right
713 chamber, or left chamber) or to that of a pair of voles (e.g., subject and right chamber
714 voles or subject and left chamber vole), resulting in continuous trajectories for each of

715 the three animals. Time in chamber was determined by the chamber location of the
716 subject vole in each frame, since the chamber location of the right chamber and left
717 chamber animals was fixed throughout the assay by physical tethering and any time the
718 contour of the subject animal merged with that of the tethered animal (right or left), the
719 subject was termed in contact with it. The algorithm also determined the boundaries of
720 the chambers and calculated chamber times. We used the chamber time data from
721 when both ends of the chamber contained tethered WTs (WT-WT condition) to ensure
722 that there was no bias in which side the choosers preferred.
723

724 ***Bond formation assays***

725 Initial introduction of Oxtr$^{1-/-}$ and WT animals of either sex with an opposite sex WT animal
726 was filmed for 30 minutes. Observed behaviors included anogenital sniffing, investigation
727 (subject animal's nose contacts any non-genital region), duration of stationary huddling
728 or >50% side-by-side contact between animals, rearing, frequency of aggressive behavior
729 including lunges, receipt of aggression, and tussles, as well as mating behavior including
730 mounting, intromission, and ejaculation. These animals remained in their home cage for
731 18 hours following pairing, after which, they were separated by a clear, plastic barrier. The
732 barrier was left in place for 24 hours and then removed allowing the subject free access
733 to the partner animal thereafter. A 30-minute period directly following barrier removal was
734 also filmed to assess mating behavior, termed the timed mating assay.
735

736 Subjects remained cohoused with the opposite-sex, wildtype partner for durations as
737 indicated in the text. The partner preference test (PPT), as previously published[52], was

738 used to assess pair bond formation. Subject, partner, and an opposite sex stranger are
739 placed in a three-chamber apparatus with open top and 10 x 32-inch walls. The partner
740 and stranger animals are tethered on either end of the three-chamber arena and the
741 subject allowed free access over a period of 3 hours. Behaviors are recorded from a top
742 view camera capturing the entire apparatus. Videos were scored using BORIS[110] post-
743 test by validated scorers blind to condition. Observed behaviors included location (i.e.,
744 duration of time in partner, stranger, and neutral chambers), duration of stationary
745 huddling or >50% side-by-side contact between the partner and stranger animals, and
746 frequency of aggressive behavior (i.e., lunges). Of note, analysis of partner preference
747 between wild type siblings from the $Oxtr^{1-/-}$ background and wild type animals from the
748 breeding colony showed no difference in time spent huddling with partner vs stranger
749 animals.
750
751 ***Bond maintenance assays***
752 Four days after the timed mating assay, female animals underwent a separation-
753 reunification assay. Females remained in their home cage while their male partners
754 were placed in a separate cage in another room for one hour. The males were then
755 reintroduced into the home cage and behavior was video recorded for 30 minutes. Male
756 subject animals underwent the same procedure five days following timed mating. Two
757 days following the separation reunification test, animals underwent a selective
758 aggression assay. Partners were again removed from the home cage and separated to
759 a separate room for an hour. After one hour, a novel sexually naïve animal of the
760 opposite sex was introduced into the home cage with the subject animal and behavior

761 observed for 20 minutes. If significant aggression occurred, defined as >3 tussles during
762 the assay, the animals were separated and the assay terminated. Overall, two WT
763 female assays and one $Oxtr^{1-/-}$ were terminated for aggression. The same behaviors
764 listed above for the introduction were observed and recorded in the reunification and
765 aggression assays.
766

767 **RNA Sequencing**

768 ***Sample collection***

769 Adult 7-9 week old WT and $Oxtr^{1-/-}$ voles were either cohoused with same sex-siblings or
770 paired with an animal of the opposite sex for four days following the timed mating protocol
771 described above. These animals were euthanized by CO_2 inhalation and decapitated. The
772 brain was quickly dissected out and sectioned into 500µm coronal slices using a brain
773 matrix mold (BrainTree Scientific) chilled on ice. Slices were floated in ice-cold phosphate
774 buffered saline (PBS), the NAc was identified using anatomical landmarks, and dissected
775 using a Zeiss microscope. A total of 45 WT females, 39 WT males, 21 $Oxtr^{1-/-}$ females,
776 and 18 $Oxtr^{1-/-}$ males were split between paired and unpaired conditions and tissue from
777 three animals per condition was pooled prior to RNA extraction. Tissue was flash-frozen
778 in liquid nitrogen and stored at -80°C until further processing. Total RNA was extracted
779 using TRIzol according to manufacturer's instructions and quantified using NanoDrop
780 (Thermo Scientific). Library preparation for next generation sequencing, comprising 35
781 samples and 4 technical replicates, was done using TruSeq Stranded mRNA Kit
782 according to manufacturer recommendations and sequenced on a NovaSeq 6000 to an

783 average depth of 2.9e07 reads per sample. Sequencing was performed across three
784 runs, but all data was processed together.
785
786 ***Read processing***
787 Adapter and low-quality sequence trimming was performed with Trimmomatic v0.39
788 using parameters: 'TruSeq3-PE.fa:2:30:10:2:keepBothReads LEADING:3 TRAILING:3
789 SLIDINGWINDOW:4:20 MINLEN:25' (Bolger et al., 2014). Trimmed RNA-Seq reads
790 were aligned to a custom MicOch1.0 prairie vole genome, which incorporated a known
791 missing gene V1A, using STAR v2.7.3a in gene annotation mode (Dobin et al., 2013).
792 Alignment, RNA-Seq, and Insert Size quality control metrics were generated using
793 Picard v 2.10.10 (http://broadinstitute.github.io/picard). Homologous genes between
794 vole, mouse, and human references were identified using biomart v2.56.1. When
795 multiple mouse or human genes mapped to the same vole gene, the homologous gene
796 with the highest percent identity to vole was selected.
797
798 ***Differential expression analysis***
799 To remove non- and lowly-expressed genes, only genes with more than 2 counts per
800 million (cpm) in at least 3 samples were retained. Principal component analysis of the
801 cpm revealed that technical replicates all cluster tightly but showed a slight batch effect
802 due to sequencing run (Fig. S5A). To remove this effect, we used RUVSeq v1.34.0 to
803 estimate one factor of unwanted variation, W_1, which we later used to normalize the
804 data prior to differential expression[111]. The factor analysis was performed on the
805 deviance residuals from an initial generalized linear model regression of the upper

806 quartile normalized counts on our covariates of interest (pair bonding status, genotype,
807 sex). Expressed genes were tested for differential expression (DE), after combining
808 technical replicates, with DESeq2 v1.40.2 using a design matrix that included the
809 covariates and W_1[112]. The adaptive shrinkage estimator ashr v2.2-63 was used in
810 order to be more robust to genes with low cpm values[113]. For DE analyses in general,
811 while most changes were driven by female samples, the effect was maintained in the
812 males at a smaller magnitude; thus, analyses were primarily performed for both sexes
813 jointly to maximize accuracy and power.
814
815 *Bonding effect*
816 To compare pre- to post-pairing individuals, we performed the DE analysis in two ways.
817 First, we compared pairing status regardless of genotype or sex to increase our
818 statistical power and to identify a reproducible gene set of thirteen genes (Fig. 5B, 5C,
819 S5B). While the relationship between the genes is unknown, there is support that the
820 proteins are functionally related. Using the STRING protein database
821 (STRINGdb_2.12.1), the human-homologs of the DE genes share more connections
822 than we would expect by chance (Fig. S5C, p-value= 3.08E-0.7). Next, we compared
823 pairing status using all three covariates, to identify subgroup-specific genes of interest
824 and effect sizes (Fig. 5D, S5D). In both analyses, genes were considered significantly
825 DE with a BH adjusted p-value < 0.05.
826

827 *Genotype effect*

828 To examine the effect of genotype, we first performed DE analyses between WT and
829 Oxtr$^{-/-}$ individuals, not including sex as a covariate to identify a reproducible and
830 stringent gene set. We considered genes DE with an adjusted p-value < 0.05 and
831 absolute log2 fold-change > 0.25 (Fig. 6B, S6A, S6B). To examine the functional
832 relationship of the DE genes, we performed a Gene Ontology enrichment analysis using
833 goseq v1.52.0 which controls for gene length bias[114]. We considered all expressed vole
834 genes with a mouse homolog as our background and all DE genes with a mouse
835 homolog as our foreground. GO categories with an adjusted p-value < 0.05 were
836 considered significantly enriched. To help visualize the results, enriched GO categories
837 were clustered according to their semantic similarity calculated with the R package
838 GOSemSim v2.26.1 using method "Wang"[115]. Large, general, GO categories with over
839 1000 genes were excluded in visualizations (Fig. 6C). WikiPathways[116] over-
840 representation analysis was performed with R package clusterProfiler v4.8.3[117] (Fig.
841 S6D).

842

843 For disorder and disease set overrepresentation analysis, Chi-squared tests were used
844 to assess whether Oxtr$^{1-/-}$ disrupted genes occur in disease-associated gene lists at a
845 frequency higher than we would expect by chance. Genes lists for autism spectrum
846 disorder[63], schizophrenia[64], neurodevelopmental disorders[66], and epilepsy[65] were
847 sourced and all alternate or outdated gene symbols were updated manually. For this
848 test, we were interested in sex- and direction-specific enrichments, so we performed a
849 DE analysis separately for males and females. Across all DE analyses, we defined DE

genes more stringently (adjusted p-value < 0.01). For enrichment tests, our universe was all expressed vole genes with a human homolog. We split this analysis by fold-change direction to highlight the distinct enrichment in upregulated genes. P-values underwent BH correction across all 24 comparisons.

To compare to mouse neuronal populations, we leveraged single-cell data on mouse hypothalamus development[72]. The released Seurat object GSE132730_subset_cca_to_velo.rds.gz was accessed at GSE132730. Using the authors' defined clusters (accessed at "prim_walktrap"), we assessed how similar each clusters' gene expression is to the genes disrupted by the $Oxtr^{1-/-}$ mutation. This was calculated as the Jaccard similarity coefficient using R package clustifyR v1.12.0[118].

Weighted Gene Coexpression Network Analysis

Data

Starting with the RNAseq dataset of n=30 samples (one WT sample and 4 replicate samples were removed) and n=13357 genes, we removed genes with low expression (n=1738 genes with expression level in lowest quantile for all 30 samples) and/or low variability (n=8230 genes with coefficient of variation < 0.05), resulting in a trimmed dataset of n=3389 genes.

Identifying co-expression modules

We used the R package WGCNA (v1.70-3) to conduct WGCNA analyses[61]. Briefly, we calculated Pearson correlations for all gene pairs. Next, we constructed an unsigned

873 weighted correlation network to identify co-expression modules comprised of highly
874 correlated genes (positive or negative correlation) with high topological overlap[119].
875 Modules were defined as branches of a hierarchical cluster tree using the top-down
876 dynamic tree cut method[61]. For each module, the expression pattern was summarized
877 by the module eigengene (ME), which is defined as the right singular vector of the
878 expression patterns. Pairs of modules with high module eigengene correlations ($r >$
879 0.75) were merged to maintain a level of decorrelation among MEs.
880
881 In more detail, a weighted unsigned network was computed based on a fit to scale-free
882 topology, and the lowest thresholding power that resulted in a scale-free R^2 fit of 0.9
883 was selected, and the pairwise topological overlap (TO) between genes was
884 calculated[119] . We constructed a TO dendrogram using hierarchical clustering (R::hclust
885 function, method= ”average”), and defined modules using the WGCNA::cutreeHybrid
886 function with minimum module size set to 30 genes. We then merged modules with high
887 module eigengene correlations as describe above.
888
889 We calculated 3 sets of modules from different sample subsets:
890 1. $Modules^{WT}$: n=15 modules constructed from n=18 WT samples with
891 thresholding power $\beta = 5$.
892 2. $Modules^{Mut}$: n= 43 modules constructed from n=12 $Oxtr^1$-mutant samples
893 with thresholding power $\beta = 6$.
894 3. $Modules^{All}$: n=7 modules constructed from all n=30 samples with
895 thresholding power $\beta = 3$

896

897 Relating modules to sample traits

898 In order to correlate modules with experimental conditions, we calculated the Pearson
899 correlations between module eigengenes and sample metrics, including species
900 (Mut=0, WT=1), condition (Pre=1, Post=0), sex (F=1, M=0), and quality control (QC)
901 metrics (RIN, yield, sequencing run). We identified three modules that significantly
902 correlated with a sample metric of interest but not with any of the QC metrics.
903 Significant correlation was defined to be $p_{adj} <= 0.05$, where p_{adj} = BH correction by
904 number of modules. These modules (M) were:

905 1. $Mpink^{WT}$: positive correlation with pre-bonding status (Pearson R = 0.7, p_{adj} =
906 0.018)
907 2. $Mbrown^{All}$: positive correlation with WT status (Pearson R = 0.55 , p_{adj} = 0.011)
908 3. $Mturquoise^{All}$: positive correlation with WT status (Pearson R = 0.8, p_{adj} = 6.6e-7)

909 We calculated the module eigengenes (ME) for $Mpink^{WT}$, $Mbrown^{All}$, and $Mturquoise^{All}$
910 for all n=30 samples using the WGCNA::moduleEigengenes function. We then
911 conducted Wilcoxon rank sum tests (ggpubr::stat_compare_means function) to assess
912 whether MEs were significantly different between the following groups:

913 1. $MEpink^{WT}$: pre- versus post-bonded animals, separated by sex and species
914 2. $Mbrown^{All}$: WT versus mutant animals, separated by sex and condition
915 3. $Mturquoise^{All}$: WT versus mutant animals, separated by sex and condition

916

917 Comparing gene significance with module membership:

918 We assessed whether genes whose expression highly correlate with module
919 eigengenes of modules of interest ($Mpink^{WT}$, $Mbrown^{All}$, and $Mturquoise^{All}$) are
920 themselves highly correlated with traits of interest (bonding status or mutation status).
921 Specifically, for the genes in $Mpink^{WT}$, $Mbrown^{All}$, and $Mturquoise^{All}$, we calculated 1)
922 gene significance (GS), defined as the absolute Pearson's correlation between
923 expression of a given gene and a trait of interest; and 2) module membership (MM),
924 which is defined as the absolute Pearson's correlation between the expression profile of
925 a gene with the ME of a module to quantify the relationship between a gene and a given
926 module[61]. We then calculated the Pearson correlations between:

927 1. $GS^{condition}$ and $MMpink^{WT}$ for $Mpink^{WT}$ genes (R = 0.69, p = 5.5e-18)
928 2. $GS^{species}$ and $MMbrown^{All}$ for $Mbrown^{All}$ genes (R = 0.63, p = 2.2e-32)
929 3. $GS^{species}$ and $MMturquoise^{All}$ for $MMturquoise^{All}$ genes (R= 0.82, p<1e-200)

930 Hub genes were defined as those genes in the top 25% for both the absolute value of
931 pink module membership and the absolute value of correlation with bonding status.
932

933 <u>Assessing whether modules are enriched for DE genes</u>

934 We were interested in assessing whether $Mpink^{WT}$ genes are significantly enriched for
935 any the DE pre vs post pairing gene set described above. We assessed for enrichment
936 of DE gene sets using a hypergeometric test.
937

938 <u>WT module preservation analysis (Zsummary)</u>

939 We assessed how well $modules^{WT}$ are preserved in mutant samples. We calculated a
940 $Z_{summary}$ statistic for each $module^{WT}$ [120] using the WGCNA::modulePreservation function

941 with 200 permutations. The $Z_{summary}$ measure combines module density and
942 intramodular connectivity metrics to a composite statistic where Z>2 suggests moderate
943 preservation and Z>10 suggests high preservation. We found of all the n=15
944 modules^{WT}, Mpink^{WT} had the lowest $Z_{summary}$ ($Z_{summary}$=2) in mutant samples.
945

946 **Histology**

947 ***Immunohistochemistry (IHC)***

948 Sexually naïve voles group housed by sex after weaning (P0, P21, adults:10 - 14 weeks
949 old), were perfused with 25mL ice cold phosphate buffer (PBS) and fixed in 25mL of 4%
950 paraformaldehyde in PBS (PFA). Whole brain was dissected and post fixed overnight at
951 4°C in 4% PFA in the dark. The tissue was cryoprotected for 24 hours in 30% sucrose in
952 PBS and then embedded in OCT over dry ice to prevent cracking. 60µm serial sections
953 from the entire PVN were collected in PBS and processed as free-floating sections.
954 Sections were blocked using 10% donkey serum in 0.1% Triton X 100 in PBS and then
955 stained with primary antibodies (Oxytocin Polyclonal Antibody, Invitrogen, Rabbit
956 Polyclonal, Cat #PA5-26701, 1:1000 and Anti-Neurophysin 2/NP-AVP Antibody, clone
957 PS 41, Millipore Sigma, Mouse Monoclonal, Cat#MABN845, 1:10,000) in 1% donkey
958 serum with 0.1% Triton X 100 (staining buffer) in PBS at 4°C with shaking. The sections
959 were rinsed and soaked in secondary antibodies (Cy™3 AffiniPure Donkey Anti-Rabbit
960 IgG, Jackson ImmunoResearch Laboratory, Cat #711-165-152, 1:500 and Alexa Flour
961 488 Donkey Anti Mouse IgG, Thermo Fisher Scientific, Cat #A21202, 1:500) in staining
962 buffer for 2 hours at room temperature. Sections were DAPI stained and transferred to
963 glass slides in sequence and mounted in Aquamount. Slides were imaged using a

964 confocal microscope (Zeiss LSM 700) and the zstacks were quantified (cell count by
965 hand and area hand selected and measured) in ImageJ. Comparisons of cell density
966 (count/area) were made in age and sex matched samples.
967

968 ***In situ hybridization (ISH)***

969 ISH was performed using RNA probes prepared as described previously[121], to detect
970 expression of *Calcr, Dlk1*, and *Dgkb* mRNA in the adult vole brain. We prepared RNA
971 sense and anti-sense probes corresponding to 706bp (CalcR), 773bp (Dgkb), and
972 796bp (Dlk1) for genes of interest identified in the WT vs Oxtr DEX list from our RNAseq
973 data. For ISH on adult animals, 7-9 week old WT and Oxtr$^{1-/-}$ voles of both sexes were
974 either group housed with same sex conspecifics or paired for 4 days with a WT animal
975 of the opposite sex following the timed mating protocol described above. The brains
976 were processed as described for IHC, then embedded in OCT and sectioned at 50µm,
977 mounted immediately after sectioning onto SuperFrost Plus glass microscope slides
978 and stored at -80°C until ISH staining. Slides were fixed in 4% PFA for 20 minutes,
979 rinsed in PBS, treated with proteinase K (10µg/mL, Roche) for 20 minutes, rinsed in
980 PBS, and fixed again in 4% PFA for 5 minutes at room temperature. Slides were
981 acylated for 10 mins then rinsed in 1% Triton100X in PBS followed by PBS. The slides
982 were equilibrated in warm hybridization solution for 1-2 hours at 65°C and subsequently
983 incubated with a temporary paraffin cover for 14 - 18 hours at 65°C in fresh
984 hybridization buffer containing RNA probe. After incubation, the slides were dipped in
985 5X SSC warmed to 72°C to remove the parafilm coverslips and then washed in 0.2X
986 SSC warmed to 72°C. The slides were blocked with 10% heat inactivated sheep serum

987 (HISS) solution then stained for 12 - 18 hours at 4°C in buffer containing 10% HISS and
988 alkaline phosphatase-conjugated sheep anti- digoxigenin antibody (1:2000, Roche).
989 After extensive washing, the slides were incubated for ~72 hours at 37°C in staining
990 solution containing nitro blue tetrazolium and 5- bromo-4-chloro-3-indolyl-phosphate
991 (Roche). The slides were finally washed, fixed in 4% PFA, and coverslipped. Slides
992 were imaged using a Keyence fluorescence microscope and the z-stacks were
993 quantified (cell count and area) in ImageJ. For signal quantitation, positive puncta were
994 counted in every third coronal section encompassing the entire anterior to posterior
995 gene expression domain. Cell counts were normalized by total area for a gene
996 expression domain in each section. Positive signal was quantified by calculating total
997 area of signal multiplied by the average intensity of signal (total area x mean pixel
998 intensity) in gene expression domains of a section; every third section was quantified
999 and added. Comparisons of cell counts were made in age and sex matched samples.

1000 **Quantification and Behavioral Analysis**

1001 For detailed statistical methods please see Table S1. The number of animals used was
1002 based on previous studies in the field by our group and others, combined with a power
1003 analysis. Assumptions of independence and normality were considered with multiple
1004 tests. Preference index (PI) was calculated as (partner huddle duration – stranger huddle
1005 duration)/(partner huddle duration + stranger huddle duration). Sliding partner preference
1006 was calculated by calculating PI for a single animal in 20-minute intervals where each
1007 interval overlapped the next by 15 minutes (e.g. 0-20mins, 5-25mins…). To look at
1008 convergence in sliding PI the area under the curve (Area above 0 – Area below 0, AUC)
1009 for each hour of the assay was determined for each animal and then pooled for each

1010 choosing animal by sex and then condition. Preference was determined as significantly
1011 convergent if the AUC from the hour of assay for all animals within the group significantly
1012 differed from 0 using a One sample t Test. The level of statistical significance for each test
1013 was set at $p =< 0.05$. Outliers were detected using a combination of z-score (+/- 3) and
1014 plots of original and log-transformed data. Analyses were completed in RStudio (version
1015 2024.04.2+764) and GraphPad Prism (version 10.3.1)
1016

1017 **FIGURE LEGENDS**

1018 **Figure1: Oxtr reduces the amount of time naive animals take to show partner**
1019 **preference**

1020 A. Schematic of the partner preference tests (PPTs) and the day on which they were
1021 conducted to study pair bonding behaviors. The prosocial, agonistic and mating
1022 behaviors scored are shown below. During the bond formation phase, the ratio of
1023 partner-directed vs stranger-directed affiliative behaviors increases in wild types
1024 and following the bond formation in the bond maintenance phase, wild types show
1025 decreased prosocial behaviors and increased agonistic behaviors towards
1026 strangers.
1027 B. A preference for partner is induced in the WTs but not $Oxtr^{1-/-}$ animals following
1028 short cohabitation.
1029 C. WT females spend more time huddling with their partners.
1030 D. $Oxtr^{1-/-}$ females spend more time huddling with strangers.
1031 E. WT females show a significant increase in partner huddling time towards the end
1032 of a 3-hour assay.

1033 F. Oxtr$^{1-/-}$ males show a significant increase in stranger huddling time in the middle of
1034 a 3-hour assay.

1035 G. No difference in partner huddling time between WT and Oxtr$^{1-/-}$ animals following
1036 long cohabitation.

1037 H. No difference in stranger huddling time between WT and Oxtr$^{1-/-}$ animals following
1038 long cohabitation.

1039 See Supplementary Figure 1 and Supplementary Table 1.

1040 Mean +/- SD, n =>8, *p =< 0.05, FWT = female WT, FOxtr$^{1-/-}$ = female Oxtr$^{1-/-}$, MWT =
1041 male WT, MOxtr$^{1-/-}$ = male Oxtr$^{1-/-}$.

1042 **Figure2: Oxtr suppresses promiscuous behaviors in a state dependent manner in**
1043 **females**

1044 A. Timeline of the behavioral battery carried out on females. Bottom row shows the
1045 behaviors scored.

1046 B. Oxtr$^{1-/-}$ female long huddle duration is shorter with partners and longer with
1047 strangers after a short cohabitation.

1048 C. Oxtr$^{1-/-}$ female long huddle frequency is greater with strangers, but not partners
1049 after a short cohabitation.

1050 D. No difference in median long huddle durations between WT and Oxtr$^{1-/-}$ females
1051 post long cohabitation.

1052 E. No difference in long huddle frequencies between WT and Oxtr$^{1-/-}$ females post
1053 long cohabitation.

1054 F. Increasing cohabitation time increases the median long huddle duration an Oxtr$^{1-/-}$
1055 female executes with the partner.
1056 G. There is no significant change in the median long huddle duration conducted by
1057 females with strangers when cohabitation time is increased.
1058 H. Naive Oxtr$^{1-/-}$ and WT females are equally prosocial towards a naive WT male.
1059 I. There is no difference in the counts of mating behaviors between Oxtr$^{1-/-}$ and WT
1060 females.
1061 J. Oxtr$^{1-/-}$ and WT females are equally prosocial towards their partners after a brief
1062 separation.
1063 K. Oxtr$^{1-/-}$ females are significantly more prosocial towards a naive WT stranger male
1064 compared to WT females.
1065 See Supplementary Figure 2 and Supplementary Table 1.
1066 Mean ± SD, n =>8, *$p < 0.05$, FWT = female WT, FOxtr$^{1-/-}$ = female Oxtr$^{1-/-}$, MWT = male
1067 WT, MOxtr$^{1-/-}$ = male Oxtr$^{1-/-}$.
1068 **Figure3: Oxtr function influences different prosocial behaviors across pair**
1069 **bonding in males**
1070 A. Timeline of the behavioral battery carried out on males. Bottom row shows the
1071 behaviors scored.
1072 B. Oxtr$^{1-/-}$ male long huddle duration is shorter with partners and strangers after a
1073 short cohabitation.
1074 C. Oxtr$^{1-/-}$ male long huddle frequency is greater with strangers, but not partners after
1075 a short cohabitation.

1076 D. The median long huddle executed by Oxtr$^{1-/-}$ males with the stranger after a long
1077 cohabitation, is shorter than their WT siblings.
1078 E. No difference in the long huddle frequencies between WT and Oxtr$^{1-/-}$ males post
1079 long cohabitation.
1080 F. There is no change in the frequency of long huddles with partner between Oxtr$^{1-/-}$
1081 and WT males.
1082 G. Increasing cohabitation time decreases the frequency of long huddles with
1083 strangers in Oxtr$^{1-/-}$ males.
1084 H. Naive Oxtr$^{1-/-}$ and WT males are equally prosocial towards naive WT females.
1085 I. Oxtr$^{1-/-}$ males execute higher counts of mating behaviors compared to WT.
1086 J. Prosocial behaviors following a brief separation with their partner are not different
1087 between Oxtr$^{1-/-}$ and WT males.
1088 K. Oxtr$^{1-/-}$ males are significantly more prosocial towards a naive WT stranger female
1089 compared to WT males.
1090 See Supplementary Figure 3 and Supplementary Table 1.
1091 Mean +/- SD, n =>8, *p =< 0.05, FWT = female WT, FOxtr$^{1-/-}$ = female Oxtr$^{1-/-}$, MWT =
1092 male WT, MOxtr$^{1-/-}$ = male Oxtr$^{1-/-}$
1093 **Figure4: Oxtr sex-specifically influences social interactions between potential**
1094 **mates**
1095 A. Schematic of naive social choice with a naive WT animal choosing between an
1096 opposite sex WT and opposite sex Oxtr$^{1-/-}$ animal (red triangles).
1097 B. Male WT choosers prefer WT females.

1098 C. Preference for WT females over Oxtr$^{1-/-}$ females by WT males manifests during
1099 the middle of a 6-hour assay.
1100 D. Schematic of comparison of time in contact with the MOAT from WT-Oxtr$^{1-/-}$
1101 condition to contact with the MOAT from WT-WT condition.
1102 E. WT female chooser spends more time in contact with a MOAT from a WT-Oxtr$^{1-/-}$
1103 condition than the WT-WT. The color of the dots represents the genotype of the
1104 MOAT.
1105 F. WT female choosers transition between contacts more frequently in the WT-WT
1106 condition compared to the WT-Oxtr$^{1-/-}$ condition.
1107 G. WT female chooser spend significantly more time in contact with the MOAT from
1108 the WT-Oxtr$^{1-/-}$ condition in the last 40 mins of the assay.
1109 H. WT female choosers prefer their MOAT over longer periods of time in the WT-
1110 Oxtr$^{1-/-}$ condition. WT male choosers prefer their MOAT earlier in the WT-Oxtr$^{1-/-}$
1111 condition, but then show preference for the same amount of time as the WT-WT.

1112 See Supplementary Figure 4 and Supplementary Table 1.
1113 Mean +/- SD, n = 8, *p =< 0.05, FWT = female WT, FOxtr$^{1-/-}$ = female Oxtr$^{1-/-}$, MWT = male
1114 WT, MOxtr$^{1-/-}$ = male Oxtr$^{1-/-}$

1115 **Figure 5: Post pair bonding gene expression is driven by female specific changes**
1116 **dependent on Oxtr signaling**

1117 A. Schematic of experimental groups used for sequencing highlighting pre- vs post-
1118 pairing comparisons between groups. Animals with symbols represent those used
1119 for tissue collection.

1120 B. Scatterplot illustrating the relationship between fold change and mean expression,
1121 emphasizing the 13 differentially expressed (DE) genes in post-pairing individuals
1122 compared to pre-pairing. Gray dots indicate non-significant genes ($p_{adj} > 0.05$);
1123 Blue dots indicate downregulated genes ($p_{adj} < 0.05$, $log_2FC < 0$) and upregulated
1124 genes in red ($p_{adj} < 0.05$, $log_2FC > 0$). The right panel shows box plots of normalized
1125 gene expression for the top six DE genes by fold-change between pre- and post-
1126 pairing conditions.
1127 C. Bar graph emphasizing how each combination of genotype and sex (denoted at
1128 bottom as 'subgroup') influence the 13 overall pairing-DE genes identified. The top
1129 graph depicts the absolute fold change and standard error of the differential
1130 expression analysis including all pre- and post-bonding individuals in which the 13
1131 genes of the x axis were identified. The bottom graph depicts the absolute fold
1132 change and standard error in analyses when only individuals of that subgroup were
1133 considered. (* denotes $p_{adj} < 0.05$ for the pre- vs post-pairing analysis).
1134 D. Box plots of select genes that show sex- and genotype-specific changes in
1135 expression with pairing condition. *Adora2A* and *Fkbp5* are DE when considering
1136 WT females, *Spred3* is DE when considering WT and $Oxtr^{1-/-}$ females, and *Sema3b*
1137 is DE when considering $Oxtr^{1-/-}$ males. Note: Sema3b is the mouse ortholog gene
1138 symbol for vole gene "ENSMOCG00000019704" which does not have an assigned
1139 gene symbol.
1140 E. Heatmap showing correlations between module eigengenes (MEs) for $modules^{WT}$
1141 and pairing condition (Pre=1, Post=0). Heatmap color and value reflect Pearson

1142 correlation coefficient; adjusted p values shown in parentheses (p_{adj} = p * number
1143 of modules).
1144 F. Preservation of modules^{WT} in OXTR-mutant samples. The $Z_{summary}$ measure
1145 combines module density and intramodular connectivity metrics to a composite
1146 statistic where Z>2 suggests moderate preservation and Z>10 suggests high
1147 preservation[119]. Of all modules^{WT}(n=15), Mpink^{WT} had the lowest $Z_{summary}$
1148 ($Z_{summary}$=2) in mutant samples.
1149 G. Box plots showing comparison of MEpink^{WT} for pre- vs post-pairing condition
1150 separated by sex and genotype. (Wilcoxon rank sum test, Bonferroni adjusted for
1151 4 comparisons).
1152 For all box plots center = median, box boundaries = 1st and 3rd quartile, whiskers =
1153 1.5*IQR from boundaries. (*n* = 16 pre-pairing and 15 post-pairing)
1154 See Supplementary Figure 5.
1155 **Figure 6: Oxtr regulated genes are common to social behavior relevant processes**
1156 **across species and are similarly regulated across brain regions**
1157 A. Schematic of experimental groups for sequencing, highlighting genotype
1158 comparisons between groups. Animals with symbols represent those used for
1159 tissue collection.
1160 B. Scatterplot illustrating the relationship between fold change and mean expression,
1161 emphasizing differentially expressed (DE) genes in Oxtr$^{1-/-}$ individuals compared
1162 to WT. Significantly downregulated genes are shown in blue ($log_2FC<-0.25$,
1163 $p_{adj}<0.05$) and upregulated genes in red ($log_2FC>0.25$, $p_{adj} < 0.05$). Box plots of

1164 normalized gene expression for the top six DE genes by fold change between
1165 genotypes.

1166 C. Gene Ontology enrichment analysis for all genotype-DE genes (n=1014) highlights
1167 processes related to extracellular channel binding activity, axonal processes,
1168 behavior related gene expression, and cation transport. The leaves represent
1169 significant GO categories (BH adjusted p value < 0.05) which have been
1170 hierarchically clustered by their semantic similarity. Branches are colored by
1171 cluster and high-frequency words are displayed to the right. Leaf size and color
1172 correspond to the number and median fold change of DE genes in each category.

1173 D. Enrichment analysis shows that genes which are DE in Oxtr$^{1-/-}$ samples are over-
1174 represented in some neuropsychiatric disease-associated gene sets. The first DE
1175 gene set evaluated ('Joint') represents genes which are DE in Oxtr$^{1-/-}$ samples
1176 when considering both sexes in the differential expression analysis ($p_{adj} < 0.01$).
1177 The second gene set are DE genes when only considering females, and the third
1178 when only considering males. Gene sets are further separated by direction of effect
1179 across the x-axis to highlight the enrichment in upregulated DE genes. Colors
1180 correspond to the Benjamini-Hochberg corrected Chi-square p values; asterisks
1181 denote $p_{adj} < 0.05$. Y-axis abbreviations are as follows: SCZ=schizophrenia,
1182 NDD=neurodevelopmental disorder, EPI=epilepsy, and ASD=autism spectrum
1183 disorder.

1184 E. Box plots of *Calcr* and *dlk1* normalized gene counts by genotype. Log_2FC:-0.962
1185 and p_{adj}: 1.75e-06 for *Calcr* and log_2FC: -0.276 and p_{adj}: 0.00334 for *dlk1* from
1186 comparison considering all WT and Oxtr$^{1-/-}$ samples.

1187 F. Brain regions selected for in situ analysis. (NAc=nucleus accumbens,
1188 PVN=paraventricular nucleus of the hypothalamus, LS=lateral septum)
1189 G. ISH images and quantification for *Calcr* expression in NAc, PVN, and LS from WT
1190 and $Oxtr^{1-/-}$ animals.
1191 H. ISH images and quantification for *Dlk-1* expression in NAc, PVN, and LS from WT
1192 and $Oxtr^{1-/-}$ animals.
1193 Box plots in G. and H. show comparison of the area-normalized cell number by
1194 genotype. (*n*=3 per condition, Wilcoxon sign rank, *=p<0.05, ***=p<0.001)
1195 See Supplementary Figure 6 and Supplementary Table 1.

1196 **Figure7: Loss of Oxtr results in the decrease in density of Oxt and Avp**
1197 **expressing neurons in the PVN**

1198 A. UMAP visualization of mouse hypothalamus single-cell RNAseq dataset[66] with
1199 proposed PVN clusters labeled. The authors' original numeric cluster labels and
1200 embedding are shown. Each cluster is colored by the Jaccard similarity coefficient
1201 between the mouse marker gene sets and the vole $Oxtr^{1-/-}$ DE genes (ONP set).
1202 This is also represented in a heat plot to the right. Some of the highest similarity is
1203 seen in Cluster 43, which represents Oxt+ cells, and Cluster 26, which represents
1204 Avp+ cells in the PVN.
1205 B. Representative images of IHC staining against OT and AVP neuropeptides from
1206 FWT and $FOxtr^{1-/-}$ PVN showing the loss of structural integrity and OT and AVP
1207 positive cells from the knock-out. (White dotted line denotes the PVN area, scale
1208 bar represents 100μm)

1209 C. Mean of positive cells per unit area across all sections is lower for Oxtr$^{1-/-}$s vs WT
1210 for both OT (left) and AVP (right). Each dot represents 1 animal.
1211 D. The number of sections with a high density of OT positive cells is greater in both
1212 female (left) and male (right) WT animals.
1213 E. Similarly, WT animals of both sexes show an increase in the number of sections
1214 containing AVP positive neurons in high densities.
1215 F. The average OT cell density from matched PVN sections arranged from anterior
1216 to posterior shows that the decrease in cell density in Oxtr$^{1-/-}$ animals is biased
1217 towards the anterior. Each dot represents the average cell density, the lines
1218 represent the sixth order non-linear regression model for cell density by sex and
1219 by genotype (n=3) and the ribbons represent the standard deviation.
1220 G. Oxtr$^{1-/-}$ animals show a significant decrease in AVP cell density in the anterior PVN
1221 in both sexes.
1222 See Supplementary Figure 7 and Supplementary Table 1.
1223 Mean +/- SD, n = 3, *p =< 0.05, FWT = female WT, FOxtr$^{1-/-}$ = female Oxtr$^{1-/-}$, MWT = male
1224 WT, MOxtr$^{1-/-}$ = male Oxtr$^{1-/-}$.
1225
1226

1227 **References**

1228

1229 1. Wilson, R.S., Krueger, K.R., Arnold, S.E., Schneider, J.A., Kelly, J.F., Barnes, L.L.,
1230 Tang, Y., and Bennett, D.A. (2007). Loneliness and Risk of Alzheimer Disease. Arch
1231 Gen Psychiatry *64*, 234. https://doi.org/10.1001/archpsyc.64.2.234.

2. Bowlby, J., and Bowlby, J. (1982). Attachment 2. ed. (Basic Books).

3. Farinelli, M., Cevolani, D., Gestieri, L., Romaniello, C., Maffei, M., Agati, R., Leo, M.R., Huang, Z., Pedone, V., and Northoff, G. (2020). Brain and behaviour in post-acute stroke: Reduction in seeking and posterior cingulate neuronal variability. Journal of Clinical and Experimental Neuropsychology *42*, 584–601. https://doi.org/10.1080/13803395.2020.1780417.

4. Feldman, R., Monakhov, M., Pratt, M., and Ebstein, R.P. (2016). Oxytocin Pathway Genes: Evolutionary Ancient System Impacting on Human Affiliation, Sociality, and Psychopathology. Biological Psychiatry *79*, 174–184. https://doi.org/10.1016/j.biopsych.2015.08.008.

5. Ebstein, R.P., Israel, S., Chew, S.H., Zhong, S., and Knafo, A. (2010). Genetics of human social behavior. Neuron *65*, 831–844. https://doi.org/10.1016/j.neuron.2010.02.020.

6. Winslow, J.T., Shapiro, L., Carter, C.S., and Insel, T.R. (1993). Oxytocin and complex social behavior: species comparisons. Psychopharmacol Bull *29*, 409–414.

7. Goodson, J.L. (2013). Deconstructing sociality, social evolution and relevant nonapeptide functions. Psychoneuroendocrinology *38*, 465–478. https://doi.org/10.1016/j.psyneuen.2012.12.005.

8. Harlow, H.F., and Harlow, M.K. (1965). THE EFFECT OF REARING CONDITIONS ON BEHAVIOR. Int J Psychiatry *1*, 43–51.

9. Shultz, S., Opie, C., and Atkinson, Q.D. (2011). Stepwise evolution of stable sociality in primates. Nature *479*, 219–222.

10. Insel, T.R., Winslow, J.T., Wang, Z., and Young, L.J. (1998). Oxytocin, vasopressin, and the neuroendocrine basis of pair bond formation. Adv. Exp. Med. Biol *449*, 215–224.

11. Klatt, J.D., and Goodson, J.L. (2013). Oxytocin-like receptors mediate pair bonding in a socially monogamous songbird. Proceedings of the Royal Society B: Biological Sciences *280*, 20122396. https://doi.org/10.1098/rspb.2012.2396.

12. Ainsworth, M.S. (1979). Infant–mother attachment. American Psychologist *34*, 932–937. https://doi.org/10.1037/0003-066X.34.10.932.

13. Getz, L.L., Carter, C.S., and Gavish, L. (1981). The mating system of the prairie vole, Microtus ochrogaster: Field and laboratory evidence for pair-bonding. Behav Ecol Sociobiol *8*, 189–194. https://doi.org/10.1007/BF00299829.

14. Donaldson, Z.R. (2010). We’re the Same... but Different: Addressing Academic Divides in the Study of Brain and Behavior. Front Behav Neurosci *4*. https://doi.org/10.3389/fnbeh.2010.00041.

15. Insel, T.R., Winslow, J.T., Wang, Z.X., Young, L., and Hulihan, T.J. (1995). Oxytocin and the molecular basis of monogamy. Adv. Exp. Med. Biol *395*, 227–234.

16. Lukas, D., and Clutton-Brock, T.H. (2013). The evolution of social monogamy in mammals. Science *341*, 526–530.

17. Donaldson, Z.R., and Young, L.J. (2008). Oxytocin, vasopressin, and the neurogenetics of sociality. Science *322*, 900–904. https://doi.org/10.1126/science.1158668.

18. Bielsky, I.F., and Young, L.J. (2004). Oxytocin, vasopressin, and social recognition in mammals. Peptides *25*, 1565–1574. https://doi.org/10.1016/j.peptides.2004.05.019.

19. Nowicki, J.P., Pratchett, M.S., Walker, S.P.W., Coker, D.J., and O'Connell, L.A. (2020). Gene expression correlates of social evolution in coral reef butterflyfishes. Proceedings of the Royal Society B: Biological Sciences *287*, 20200239. https://doi.org/10.1098/rspb.2020.0239.

20. O'Connor, C.M., Marsh-Rollo, S.E., Aubin-Horth, N., and Balshine, S. (2016). Species-specific patterns of nonapeptide brain gene expression relative to pair-bonding behavior in grouping and non-grouping cichlids. Hormones and Behavior *80*, 30–38. https://doi.org/10.1016/j.yhbeh.2015.10.015.

21. Stanley, D.A., and Adolphs, R. (2013). Toward a neural basis for social behavior. Neuron *80*, 816–826.

22. Insel, T.R. (1992). Oxytocin--a neuropeptide for affiliation: evidence from behavioral, receptor autoradiographic, and comparative studies. Psychoneuroendocrinology *17*, 3–35.

23. Lim, M.M., and Young, L.J. (2006). Neuropeptidergic regulation of affiliative behavior and social bonding in animals. Horm Behav *50*, 506–517. https://doi.org/10.1016/j.yhbeh.2006.06.028.

24. Carter, C.S., and Getz, L.L. (1993). Monogamy and the prairie vole. Sci. Am *268*, 100–106.

25. Beery, A.K., and Shambaugh, K.L. (2021). Comparative assessment of familiarity/novelty preferences in rodents. Frontiers in Behavioral Neuroscience *15*, 648830.

26. Beery, A.K., Christensen, J.D., Lee, N.S., and Blandino, K.L. (2018). Specificity in Sociality: Mice and Prairie Voles Exhibit Different Patterns of Peer Affiliation. Frontiers in Behavioral Neuroscience *12*, 50. https://doi.org/10.3389/fnbeh.2018.00050.

27. Schweinfurth, M.K., Neuenschwander, J., Engqvist, L., Schneeberger, K., Rentsch, A.K., Gygax, M., and Taborsky, M. (2017). Do female Norway rats form social bonds? Behavioral Ecology and Sociobiology *71*, 1–9.

28. Cho, M.M., DeVries, A.C., Williams, J.R., and Carter, C.S. (1999). The effects of oxytocin and vasopressin on partner preferences in male and female prairie voles (Microtus ochrogaster). Behav. Neurosci *113*, 1071–1079.

29. Insel, T.R., and Hulihan, T.J. (1995). A gender-specific mechanism for pair bonding: oxytocin and partner preference formation in monogamous voles. Behav. Neurosci *109*, 782–789.

30. Williams, J.R., Catania, K.C., and Carter, C.S. (1992). Development of partner preferences in female prairie voles (Microtus ochrogaster): the role of social and sexual experience. Hormones and behavior *26*, 339–349.

1314 31. Wang, Z., Hulihan, T.J., and Insel, T.R. (1997). Sexual and social experience is
1315 associated with different patterns of behavior and neural activation in male prairie
1316 voles. Brain Res *767*, 321–332.

1317 32. Xu, X., Coats, J.K., Yang, C.F., Wang, A., Ahmed, O.M., Alvarado, M., Izumi, T., and
1318 Shah, N.M. (2012). Modular genetic control of sexually dimorphic behaviors. Cell
1319 *148*, 596–607. https://doi.org/10.1016/j.cell.2011.12.018.

1320 33. Villella, A., and Hall, J.C. (2008). Chapter 3 Neurogenetics of Courtship and Mating
1321 in Drosophila. In Advances in Genetics (Elsevier), pp. 67–184.
1322 https://doi.org/10.1016/S0065-2660(08)00603-2.

1323 34. Konopka, R.J., and Benzer, S. (1971). Clock Mutants of *Drosophila melanogaster*.
1324 Proc Natl Acad Sci USA *68*, 2112–2116. https://doi.org/10.1073/pnas.68.9.2112.

1325 35. Takahashi, J.S., Shimomura, K., and Kumar, V. (2008). Searching for genes
1326 underlying behavior: lessons from circadian rhythms. Science *322*, 909–912.
1327 https://doi.org/10.1126/science.1158822.

1328 36. Baker, B.S., Taylor, B.J., and Hall, J.C. (2001). Are complex behaviors specified by
1329 dedicated regulatory genes? Reasoning from Drosophila. Cell *105*, 13–24.

1330 37. Manoli, D.S., and Baker, B.S. (2004). Median bundle neurons coordinate behaviours
1331 during Drosophila male courtship. Nature *430*, 564–569.
1332 https://doi.org/10.1038/nature02713.

38. Martin, L.B., Glasper, E.R., Nelson, R.J., and DeVries, A.C. (2006). Prolonged separation delays wound healing in monogamous California mice, Peromyscus californicus, but not in polygynous white-footed mice, P. leucopus. Physiology & Behavior *87*, 837–841. https://doi.org/10.1016/j.physbeh.2006.01.035.

39. Ferland, C.L., and Schrader, L.A. (2011). Cage mate separation in pair-housed male rats evokes an acute stress corticosterone response. Neuroscience Letters *489*, 154–158. https://doi.org/10.1016/j.neulet.2010.12.006.

40. Okuda, T., Osako, Y., Hidaka, C., Nishihara, M., Young, L.J., Mitsui, S., and Yuri, K. (2022). Separation from a bonded partner alters neural response to inflammatory pain in monogamous rodents. Behavioural Brain Research *418*, 113650. https://doi.org/10.1016/j.bbr.2021.113650.

41. Carter, C.S., Williams, J.R., Witt, D.M., and Insel, T.R. (1992). Oxytocin and social bonding. Ann. N. Y. Acad. Sci *652*, 204–211.

42. Winslow, J.T., Hastings, N., Carter, C.S., Harbaugh, C.R., and Insel, T.R. (1993). A role for central vasopressin in pair bonding in monogamous prairie voles. Nature *365*, 545–548. https://doi.org/10.1038/365545a0.

43. Carter, C.S., Grippo, A.J., Pournajafi-Nazarloo, H., Ruscio, M.G., and Porges, S.W. (2008). Oxytocin, vasopressin and sociality. Prog. Brain Res *170*, 331–336. https://doi.org/10.1016/S0079-6123(08)00427-5.

1352 44. Ophir, A.G., Gessel, A., Zheng, D.-J., and Phelps, S.M. (2012). Oxytocin receptor
1353 density is associated with male mating tactics and social monogamy. Hormones and
1354 behavior *61*, 445–453.

1355 45. Shapiro, L.E., and Insel, T.R. (1992). Oxytocin receptor distribution reflects social
1356 organization in monogamous and polygamous voles. Ann. N. Y. Acad. Sci *652*, 448–
1357 451.

1358 46. Heinrichs, M., von Dawans, B., and Domes, G. (2009). Oxytocin, vasopressin, and
1359 human social behavior. Front Neuroendocrinol *30*, 548–557.
1360 https://doi.org/10.1016/j.yfrne.2009.05.005.

1361 47. Insel, T.R., Wang, Z.X., and Ferris, C.F. (1994). Patterns of brain vasopressin
1362 receptor distribution associated with social organization in microtine rodents. J.
1363 Neurosci *14*, 5381–5392.

1364 48. King, L.B., Walum, H., Inoue, K., Eyrich, N.W., and Young, L.J. (2016). Variation in
1365 the oxytocin receptor gene predicts brain region–specific expression and social
1366 attachment. Biological psychiatry *80*, 160–169.

1367 49. Walum, H., and Young, L.J. (2018). The neural mechanisms and circuitry of the pair
1368 bond. Nat Rev Neurosci *19*, 643–654. https://doi.org/10.1038/s41583-018-0072-6.

1369 50. Williams, J.R., Insel, T.R., Harbaugh, C.R., and Carter, C.S. (1994). Oxytocin
1370 administered centrally facilitates formation of a partner preference in female prairie
1371 voles (Microtus ochrogaster). J. Neuroendocrinol *6*, 247–250.

1372 51. Bales, K.L., and Carter, C.S. (2003). Developmental exposure to oxytocin facilitates
1373 partner preferences in male prairie voles (Microtus ochrogaster). Behavioral
1374 neuroscience *117*, 854.

1375 52. Berendzen, K.M., Sharma, R., Mandujano, M.A., Wei, Y., Rogers, F.D., Simmons,
1376 T.C., Seelke, A.M., Bond, J.M., Larios, R., Goodwin, N.L., et al. (2023). Oxytocin
1377 receptor is not required for social attachment in prairie voles. Neuron *111*, 787–796.

1378 53. Young, L.J., Lim, M.M., Gingrich, B., and Insel, T.R. (2001). Cellular mechanisms of
1379 social attachment. Hormones and behavior *40*, 133–138.

1380 54. Tripp, J.A., Berrio, A., McGraw, L.A., Matz, M.V., Davis, J.K., Inoue, K., Thomas,
1381 J.W., Young, L.J., and Phelps, S.M. (2021). Comparative neurotranscriptomics
1382 reveal widespread species differences associated with bonding. BMC Genomics *22*,
1383 399. https://doi.org/10.1186/s12864-021-07720-0.

1384 55. Young, L.J., and Wang, Z. (2004). The neurobiology of pair bonding. Nat. Neurosci
1385 *7*, 1048–1054. https://doi.org/10.1038/nn1327.

1386 56. DeVries, A.C., and Carter, C.S. (1999). Sex differences in temporal parameters of
1387 partner preference in prairie voles (Microtus ochrogaster). Can. J. Zool. *77*, 885–
1388 889. https://doi.org/10.1139/z99-054.

1389 57. Fraser, E.J., and Shah, N.M. (2014). Complex Chemosensory Control of Female
1390 Reproductive Behaviors. PLOS ONE *9*, e90368.
1391 https://doi.org/10.1371/journal.pone.0090368.

1392 58. Aragona, B.J., Liu, Y., Curtis, J.T., Stephan, F.K., and Wang, Z. (2003). A Critical
1393 Role for Nucleus Accumbens Dopamine in Partner-Preference Formation in Male
1394 Prairie Voles. J. Neurosci. *23*, 3483–3490. https://doi.org/10.1523/JNEUROSCI.23-
1395 08-03483.2003.

1396 59. Dölen, G., Darvishzadeh, A., Huang, K.W., and Malenka, R.C. (2013). Social reward
1397 requires coordinated activity of nucleus accumbens oxytocin and serotonin. Nature
1398 *501*, 179–184. https://doi.org/10.1038/nature12518.

1399 60. Ross, H.E., Freeman, S.M., Spiegel, L.L., Ren, X., Terwilliger, E.F., and Young, L.J.
1400 (2009). Variation in Oxytocin Receptor Density in the Nucleus Accumbens Has
1401 Differential Effects on Affiliative Behaviors in Monogamous and Polygamous Voles.
1402 J. Neurosci. *29*, 1312–1318. https://doi.org/10.1523/JNEUROSCI.5039-08.2009.

1403 61. Langfelder, P., and Horvath, S. (2008). WGCNA: an R package for weighted
1404 correlation network analysis. BMC Bioinformatics *9*, 559.
1405 https://doi.org/10.1186/1471-2105-9-559.

1406 62. Maury, E.A., Sherman, M.A., Genovese, G., Gilgenast, T.G., Kamath, T., Burris, S.J.,
1407 Rajarajan, P., Flaherty, E., Akbarian, S., Chess, A., et al. (2023). Schizophrenia-
1408 associated somatic copy-number variants from 12,834 cases reveal recurrent
1409 NRXN1 and ABCB11 disruptions. Cell Genom *3*, 100356.
1410 https://doi.org/10.1016/j.xgen.2023.100356.

1411 63. Satterstrom, F.K., Kosmicki, J.A., Wang, J., Breen, M.S., De Rubeis, S., An, J.-Y.,
1412 Peng, M., Collins, R., Grove, J., Klei, L., et al. (2020). Large-Scale Exome

1413 Sequencing Study Implicates Both Developmental and Functional Changes in the
1414 Neurobiology of Autism. Cell *180*, 568-584.e23.
1415 https://doi.org/10.1016/j.cell.2019.12.036.

1416 64. Fromer, M., Pocklington, A.J., Kavanagh, D.H., Williams, H.J., Dwyer, S., Gormley,
1417 P., Georgieva, L., Rees, E., Palta, P., Ruderfer, D.M., et al. (2014). De novo
1418 mutations in schizophrenia implicate synaptic networks. Nature *506*, 179–184.
1419 https://doi.org/10.1038/nature12929.

1420 65. EuroEPINOMICS-RES Consortium, Epilepsy Phenome/Genome Project, and Epi4K
1421 Consortium (2014). De novo mutations in synaptic transmission genes including
1422 DNM1 cause epileptic encephalopathies. Am J Hum Genet *95*, 360–370.
1423 https://doi.org/10.1016/j.ajhg.2014.08.013.

1424 66. Kaplanis, J., Samocha, K.E., Wiel, L., Zhang, Z., Arvai, K.J., Eberhardt, R.Y.,
1425 Gallone, G., Lelieveld, S.H., Martin, H.C., McRae, J.F., et al. (2020). Evidence for 28
1426 genetic disorders discovered by combining healthcare and research data. Nature
1427 *586*, 757–762. https://doi.org/10.1038/s41586-020-2832-5.

1428 67. Inoue, K., Ford, C.L., Horie, K., and Young, L.J. (2022). Oxytocin receptors are
1429 widely distributed in the prairie vole (Microtus ochrogaster) brain: Relation to social
1430 behavior, genetic polymorphisms, and the dopamine system. J Comp Neurol *530*,
1431 2881–2900. https://doi.org/10.1002/cne.25382.

1432 68. Lefevre, A., Benusiglio, D., Tang, Y., Krabichler, Q., Charlet, A., and Grinevich, V.
1433 (2021). Oxytocinergic Feedback Circuitries: An Anatomical Basis for

1434 Neuromodulation of Social Behaviors. Front. Neural Circuits *15*, 688234.
1435 https://doi.org/10.3389/fncir.2021.688234.

1436 69. Harris, G.W. (1955). PITUITARY-HYPOTHALAMIC MECHANISMS. Arch NeurPsych
1437 *73*, 124. https://doi.org/10.1001/archneurpsyc.1955.02330080002002.

1438 70. Ye, Q., Nunez, J., and Zhang, X. (2022). Oxytocin Receptor-Expressing Neurons in
1439 the Paraventricular Thalamus Regulate Feeding Motivation through Excitatory
1440 Projections to the Nucleus Accumbens Core. J. Neurosci. *42*, 3949–3964.
1441 https://doi.org/10.1523/JNEUROSCI.2042-21.2022.

1442 71. Zhang, B., Qiu, L., Xiao, W., Ni, H., Chen, L., Wang, F., Mai, W., Wu, J., Bao, A., Hu,
1443 H., et al. (2021). Reconstruction of the Hypothalamo-Neurohypophysial System and
1444 Functional Dissection of Magnocellular Oxytocin Neurons in the Brain. Neuron *109*,
1445 331-346.e7. https://doi.org/10.1016/j.neuron.2020.10.032.

1446 72. Romanov, R.A., Tretiakov, E.O., Kastriti, M.E., Zupancic, M., Häring, M.,
1447 Korchynska, S., Popadin, K., Benevento, M., Rebernik, P., Lallemend, F., et al.
1448 (2020). Molecular design of hypothalamus development. Nature *582*, 246–252.
1449 https://doi.org/10.1038/s41586-020-2266-0.

1450 73. Mitre, M., Saadipour, K., Williams, K., Khatri, L., Froemke, R.C., and Chao, M.V.
1451 (2022). Transactivation of TrkB Receptors by Oxytocin and Its G Protein-Coupled
1452 Receptor. Front Mol Neurosci *15*, 891537.
1453 https://doi.org/10.3389/fnmol.2022.891537.

1454 74. Seoyoung Son, Steffy B. Manjila, Kyra T. Newmaster, Yuan-ting Wu, Daniel J.
1455 Vanselow, Matt Ciarletta, Todd E. Anthony, Keith C. Cheng, and Yongsoo Kim
1456 (2022). Whole-Brain Wiring Diagram of Oxytocin System in Adult Mice. J. Neurosci.
1457 *42*, 5021. https://doi.org/10.1523/JNEUROSCI.0307-22.2022.

1458 75. Vaidyanathan, R., and Hammock, E.A.D. (2020). Oxytocin receptor gene loss
1459 influences expression of the oxytocin gene in C57BL/6J mice in a sex- and age-
1460 dependent manner. Journal of Neuroendocrinology *32*, e12821.
1461 https://doi.org/10.1111/jne.12821.

1462 76. Newmaster, K.T., Nolan, Z.T., Chon, U., Vanselow, D.J., Weit, A.R., Tabbaa, M.,
1463 Hidema, S., Nishimori, K., Hammock, E.A.D., and Kim, Y. (2020). Quantitative
1464 cellular-resolution map of the oxytocin receptor in postnatally developing mouse
1465 brains. Nature Communications *11*, 1885. https://doi.org/10.1038/s41467-020-
1466 15659-1.

1467 77. Kleiman, D.G. (1977). Monogamy in Mammals. The Quarterly Review of Biology *52*,
1468 39–69. https://doi.org/10.1086/409721.

1469 78. Feldman, R. (2017). The Neurobiology of Human Attachments. Trends in Cognitive
1470 Sciences *21*, 80–99. https://doi.org/10.1016/j.tics.2016.11.007.

1471 79. Yang, C.F., and Shah, N.M. (2014). Representing sex in the brain, one module at a
1472 time. Neuron *82*, 261–278. https://doi.org/10.1016/j.neuron.2014.03.029.

1473 80. Mong, J.A., and Pfaff, D.W. (2004). Hormonal symphony: steroid orchestration of
1474 gene modules for sociosexual behaviors. Mol Psychiatry *9*, 550–556.
1475 https://doi.org/10.1038/sj.mp.4001493.

1476 81. Mong, J., Easton, A., Kow, L.M., and Pfaff, D. (2003). Neural, hormonal and genetic
1477 mechanisms for the activation of brain and behavior. Eur J Pharmacol *480*, 229–
1478 231. https://doi.org/10.1016/j.ejphar.2003.08.109.

1479 82. Barron, A.B., and Robinson, G.E. (2008). The utility of behavioral models and
1480 modules in molecular analyses of social behavior. Genes Brain and Behavior *7*,
1481 257–265. https://doi.org/10.1111/j.1601-183X.2007.00344.x.

1482 83. Kyriacou, C.P., and Hall, J.C. (1980). Circadian rhythm mutations in Drosophila
1483 melanogaster affect short-term fluctuations in the male's courtship song. Proc Natl
1484 Acad Sci U S A *77*, 6729–6733. https://doi.org/10.1073/pnas.77.11.6729.

1485 84. Konopka, R.J., and Benzer, S. (1971). Clock Mutants of *Drosophila melanogaster*.
1486 Proc Natl Acad Sci USA *68*, 2112–2116. https://doi.org/10.1073/pnas.68.9.2112.

1487 85. Bendesky, A., Kwon, Y.-M., Lassance, J.-M., Lewarch, C.L., Yao, S., Peterson, B.K.,
1488 He, M.X., Dulac, C., and Hoekstra, H.E. (2017). The genetic basis of parental care
1489 evolution in monogamous mice. Nature *544*, 434–439.
1490 https://doi.org/10.1038/nature22074.

1491 86. Scheele, D., Striepens, N., Güntürkün, O., Deutschländer, S., Maier, W., Kendrick,
1492 K.M., and Hurlemann, R. (2012). Oxytocin modulates social distance between males

and females. J Neurosci *32*, 16074–16079. https://doi.org/10.1523/JNEUROSCI.2755-12.2012.

87. Ditzen, B., Schaer, M., Gabriel, B., Bodenmann, G., Ehlert, U., and Heinrichs, M. (2009). Intranasal Oxytocin Increases Positive Communication and Reduces Cortisol Levels During Couple Conflict. Biological Psychiatry *65*, 728–731. https://doi.org/10.1016/j.biopsych.2008.10.011.

88. De Dreu, C.K.W., Greer, L.L., Handgraaf, M.J.J., Shalvi, S., Van Kleef, G.A., Baas, M., Ten Velden, F.S., Van Dijk, E., and Feith, S.W.W. (2010). The Neuropeptide Oxytocin Regulates Parochial Altruism in Intergroup Conflict Among Humans. Science *328*, 1408–1411. https://doi.org/10.1126/science.1189047.

89. Osakada, T., Yan, R., Jiang, Y., Wei, D., Tabuchi, R., Dai, B., Wang, X., Zhao, G., Wang, C.X., Liu, J.-J., et al. (2024). A dedicated hypothalamic oxytocin circuit controls aversive social learning. Nature *626*, 347–356. https://doi.org/10.1038/s41586-023-06958-w.

90. Wang, Z., and Young, L.J. (1997). Ontogeny of oxytocin and vasopressin receptor binding in the lateral septum in prairie and montane voles. Brain Res. Dev. Brain Res *104*, 191–195.

91. Smith, M.L., Asada, N., and Malenka, R.C. (2021). Anterior cingulate inputs to nucleus accumbens control the social transfer of pain and analgesia. Science *371*, 153–159. https://doi.org/10.1126/science.abe3040.

1513 92. Gegenhuber, B., Wu, M.V., Bronstein, R., and Tollkuhn, J. (2020). Regulation of
1514 neural gene expression by estrogen receptor alpha (Neuroscience)
1515 https://doi.org/10.1101/2020.10.21.349290.

1516 93. Cao, J., and Patisaul, H.B. (2013). Sex-specific expression of estrogen receptors α
1517 and β and Kiss1 in the postnatal rat amygdala. J of Comparative Neurology *521*,
1518 465–478. https://doi.org/10.1002/cne.23185.

1519 94. Mitsushima, D., Yamada, K., Takase, K., Funabashi, T., and Kimura, F. (2006). Sex
1520 differences in the basolateral amygdala: the extracellular levels of serotonin and
1521 dopamine, and their responses to restraint stress in rats. Eur J Neurosci *24*, 3245–
1522 3254. https://doi.org/10.1111/j.1460-9568.2006.05214.x.

1523 95. McCann, K.E., Sinkiewicz, D.M., Rosenhauer, A.M., Beach, L.Q., and Huhman, K.L.
1524 (2019). Transcriptomic Analysis Reveals Sex-Dependent Expression Patterns in the
1525 Basolateral Amygdala of Dominant and Subordinate Animals After Acute Social
1526 Conflict. Mol Neurobiol *56*, 3768–3779. https://doi.org/10.1007/s12035-018-1339-7.

1527 96. Trainor, B.C. (2011). Stress responses and the mesolimbic dopamine system: social
1528 contexts and sex differences. Horm Behav *60*, 457–469.
1529 https://doi.org/10.1016/j.yhbeh.2011.08.013.

1530 97. Wright, E.C., Luo, P.X., Zakharenkov, H.C., Serna Godoy, A., Lake, A.A., Prince,
1531 Z.D., Sekar, S., Culkin, H.I., Ramirez, A.V., Dwyer, T., et al. (2023). Sexual
1532 differentiation of neural mechanisms of stress sensitivity during puberty. Proc. Natl.
1533 Acad. Sci. U.S.A. *120*, e2306475120. https://doi.org/10.1073/pnas.2306475120.

98. Dölen, G. (2015). Oxytocin: parallel processing in the social brain? J. Neuroendocrinol. *27*, 516–535. https://doi.org/10.1111/jne.12284.

99. Choi, T.-Y., Jeon, H., Jeong, S., Kim, E.J., Kim, J., Jeong, Y.H., Kang, B., Choi, M., and Koo, J.W. (2023). Distinct prefrontal projection activity and transcriptional state conversely orchestrate social competition and hierarchy. Neuron, S0896-6273(23)00886-3. https://doi.org/10.1016/j.neuron.2023.11.012.

100. Yaguchi, K., Hagihara, M., Konno, A., Hirai, H., Yukinaga, H., and Miyamichi, K. (2023). Dynamic modulation of pulsatile activities of oxytocin neurons in lactating wild-type mice. PLoS One *18*, e0285589. https://doi.org/10.1371/journal.pone.0285589.

101. Manoli, D.S., and State, M.W. (2021). Autism Spectrum Disorder Genetics and the Search for Pathological Mechanisms. AJP *178*, 30–38. https://doi.org/10.1176/appi.ajp.2020.20111608.

102. Werling, D.M. (2016). The role of sex-differential biology in risk for autism spectrum disorder. Biology of Sex Differences *7*, 58. https://doi.org/10.1186/s13293-016-0112-8.

103. Werling, D.M., and Geschwind, D.H. (2013). Sex differences in autism spectrum disorders. Curr. Opin. Neurol. *26*, 146–153. https://doi.org/10.1097/WCO.0b013e32835ee548.

1553 104. Perissi, V., and Rosenfeld, M.G. (2005). Controlling nuclear receptors: the
1554 circular logic of cofactor cycles. Nature Reviews: Molecular Cell Biology *6*, 542–554.
1555 https://doi.org/10.1038/nrm1682.

1556 105. Horie, K., Inoue, K., Nishimori, K., and Young, L.J. (2020). Investigation of Oxtr-
1557 expressing Neurons Projecting to Nucleus Accumbens using Oxtr-ires-Cre Knock-in
1558 prairie Voles (Microtus ochrogaster). Neuroscience *448*, 312–324.
1559 https://doi.org/10.1016/j.neuroscience.2020.08.023.

1560 106. Villanueva, C., Jacquier, S., and de Roux, N. (2012). DLK1 Is a Somato-Dendritic
1561 Protein Expressed in Hypothalamic Arginine-Vasopressin and Oxytocin Neurons.
1562 PLoS One *7*, e36134. https://doi.org/10.1371/journal.pone.0036134.

1563 107. Insel, T.R. (1997). A neurobiological basis of social attachment. Am J Psychiatry
1564 *154*, 726–735.

1565 108. Carter, C.S., and Perkeybile, A.M. (2018). The Monogamy Paradox: What Do
1566 Love and Sex Have to Do With It? Front. Ecol. Evol. *6*, 202.
1567 https://doi.org/10.3389/fevo.2018.00202.

1568 109. De Vries, G.J. (2004). Minireview: Sex Differences in Adult and Developing
1569 Brains: Compensation, Compensation, Compensation. Endocrinology *145*, 1063–
1570 1068. https://doi.org/10.1210/en.2003-1504.

1571 110. Friard, O., and Gamba, M. (2016). BORIS: a free, versatile open-source event-
1572 logging software for video/audio coding and live observations. Methods in ecology
1573 and evolution *7*, 1325–1330.

1574 111. Risso, D., Ngai, J., Speed, T.P., and Dudoit, S. (2014). Normalization of RNA-seq
1575 data using factor analysis of control genes or samples. Nat Biotechnol *32*, 896–902.
1576 https://doi.org/10.1038/nbt.2931.

1577 112. Love, M.I., Huber, W., and Anders, S. (2014). Moderated estimation of fold
1578 change and dispersion for RNA-seq data with DESeq2. Genome Biol *15*, 550.
1579 https://doi.org/10.1186/s13059-014-0550-8.

1580 113. Stephens, M., Carbonetto, P., Gerard, D., Lu, M., Sun, L., Willwerscheid, J., and
1581 Xiao, N. (2020). Methods for Adaptive Shrinkage, using Empirical Bayes [R package
1582 ashr version 2.2-47]. In.

1583 114. Young, M.D., Wakefield, M.J., Smyth, G.K., and Oshlack, A. (2010). Gene
1584 ontology analysis for RNA-seq: accounting for selection bias. Genome Biol *11*, R14.
1585 https://doi.org/10.1186/gb-2010-11-2-r14.

1586 115. Yu, G. (2020). Gene Ontology Semantic Similarity Analysis Using GOSemSim. In
1587 Stem Cell Transcriptional Networks Methods in Molecular Biology., B. L. Kidder, ed.
1588 (Springer US), pp. 207–215. https://doi.org/10.1007/978-1-0716-0301-7_11.

1589 116. Pico, A.R., Kelder, T., Van Iersel, M.P., Hanspers, K., Conklin, B.R., and Evelo, C.
1590 (2008). WikiPathways: Pathway Editing for the People. PLoS Biol *6*, e184.
1591 https://doi.org/10.1371/journal.pbio.0060184.

1592 117. Wu, T., Hu, E., Xu, S., Chen, M., Guo, P., Dai, Z., Feng, T., Zhou, L., Tang, W.,
1593 Zhan, L., et al. (2021). clusterProfiler 4.0: A universal enrichment tool for interpreting
1594 omics data. The Innovation *2*, 100141. https://doi.org/10.1016/j.xinn.2021.100141.

1595 118. Fu, R., Gillen, A.E., Sheridan, R.M., Tian, C., Daya, M., Hao, Y., Hesselberth,
1596 J.R., and Riemondy, K.A. (2020). clustifyr: an R package for automated single-cell
1597 RNA sequencing cluster classification. F1000Res *9*, 223.
1598 https://doi.org/10.12688/f1000research.22969.2.

1599 119. Zhang, B., and Horvath, S. (2005). A general framework for weighted gene co-
1600 expression network analysis. Stat Appl Genet Mol Biol *4*, Article17.
1601 https://doi.org/10.2202/1544-6115.1128.

1602 120. Langfelder, P., Luo, R., Oldham, M.C., and Horvath, S. (2011). Is my network
1603 module preserved and reproducible? PLoS Comput Biol *7*, e1001057.
1604 https://doi.org/10.1371/journal.pcbi.1001057.

1605 121. Gandrillon, O., Solari, F., Legrand, C., Jurdic, P., and Samarut, J. (1996). A rapid
1606 and convenient method to prepare DIG-labelled RNA probes for use in non-
1607 radioactive in situ hybridization. Molecular and cellular probes *10*, 51–56.

1608

Figure 1: Oxtr reduces the amount of time naïve animals take to show partner preference

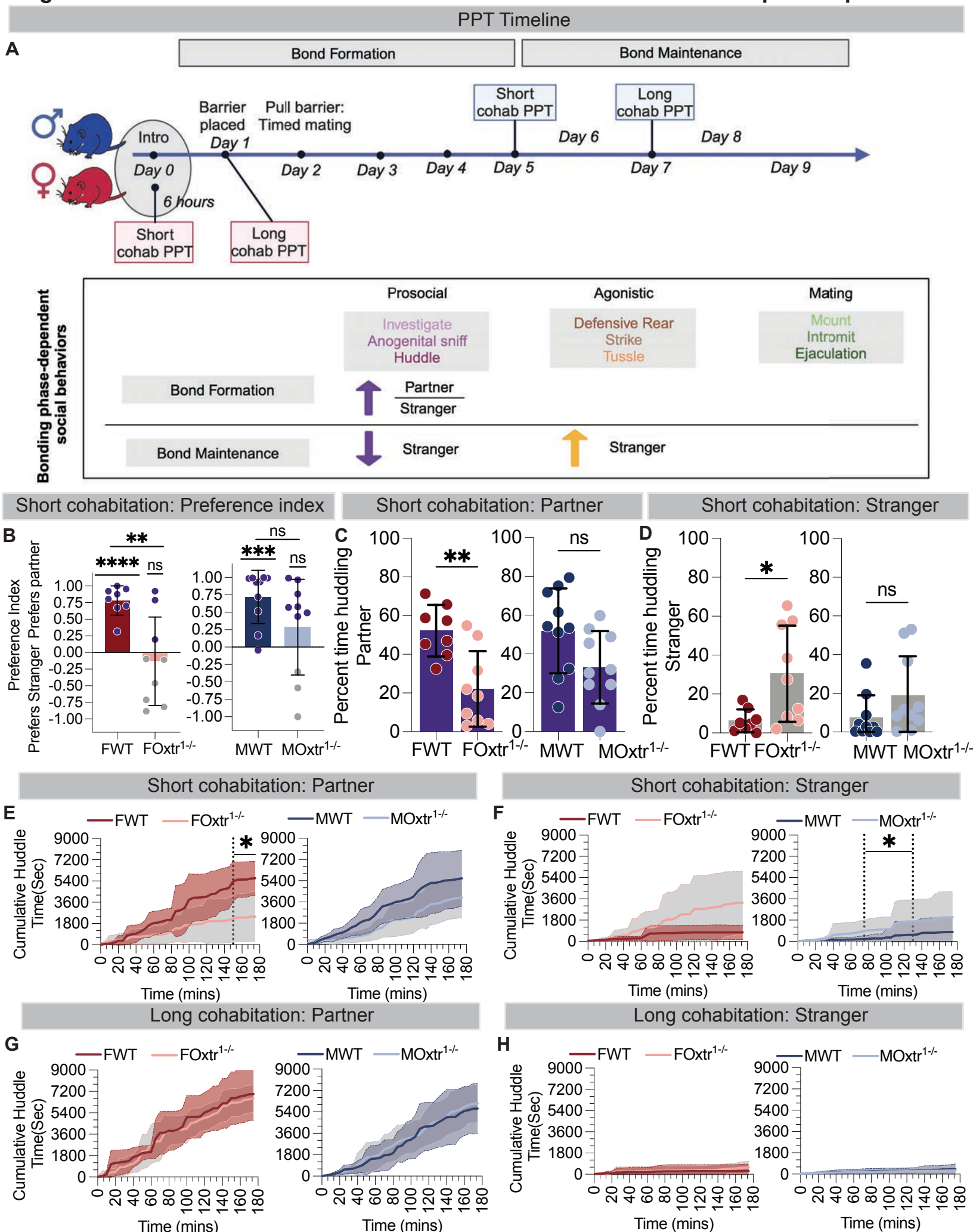

Figure 2: Oxtr suppresses promiscuous behaviors in a state dependent manner in females

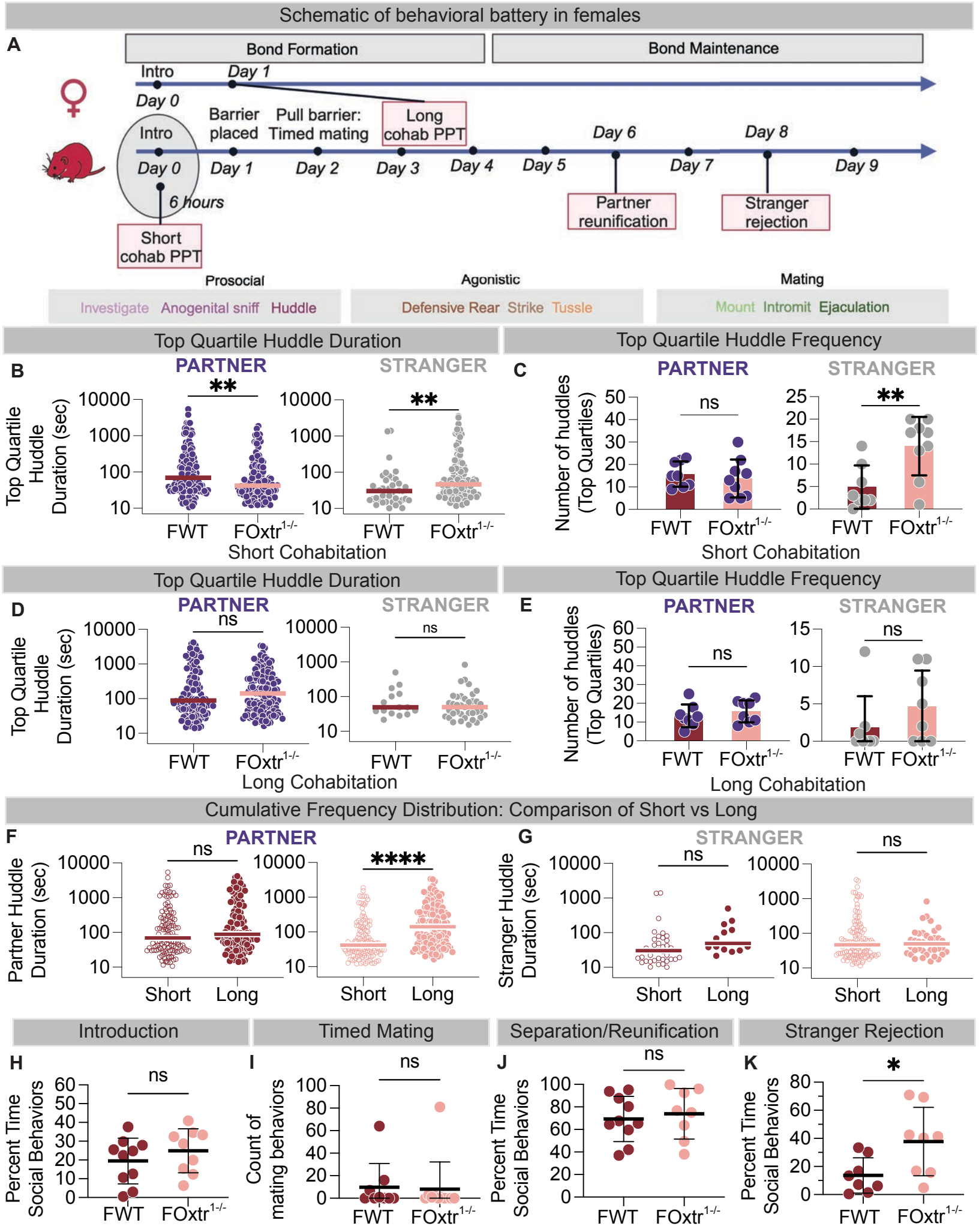

Figure 3: Oxtr function influences different prosocial behaviors across pair bonding in males

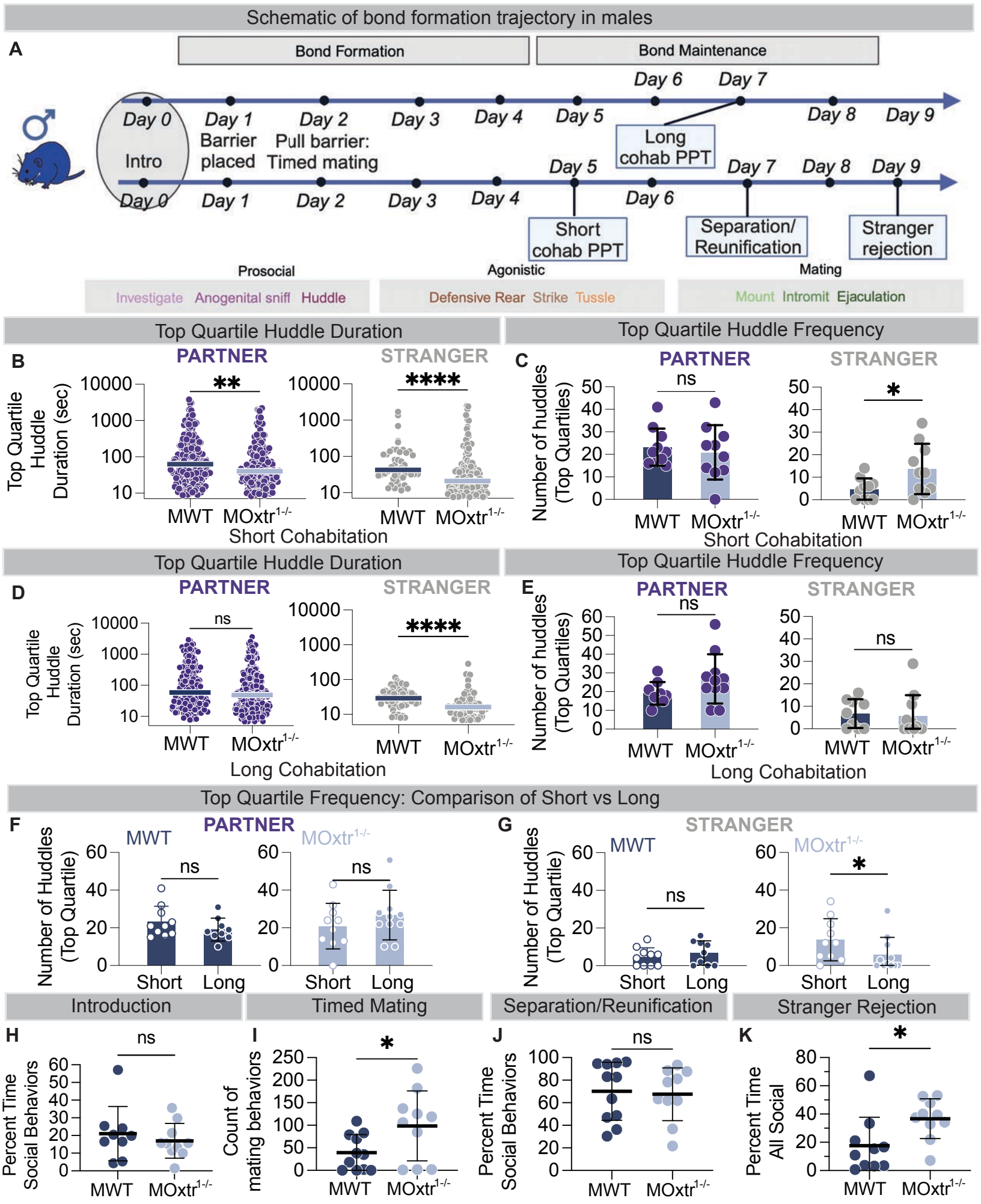

Figure 4: Oxtr sex-specifically influences social interactions between potential mates

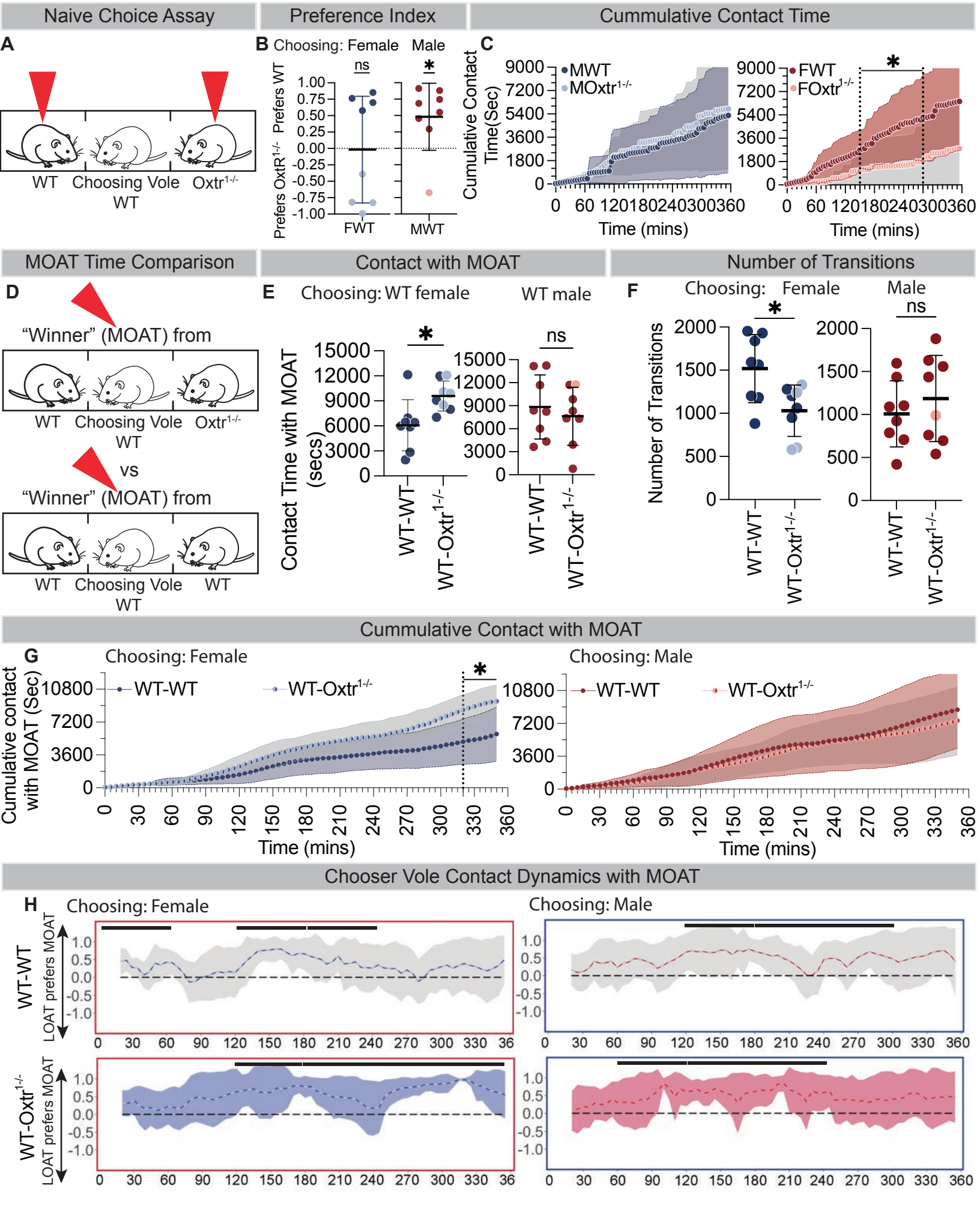

Figure 5: Post pair bonding gene expression is driven by female specific changes dependent on Oxtr signaling

Comparison groups for sequencing

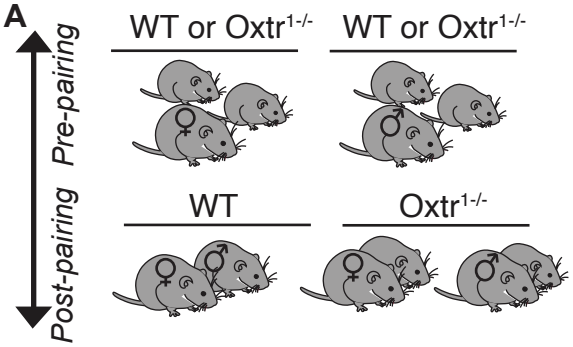

Pre- vs Post-pairing DE genes

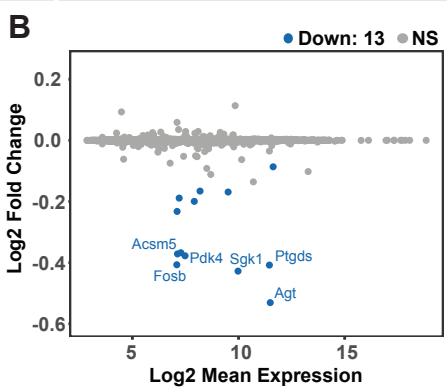

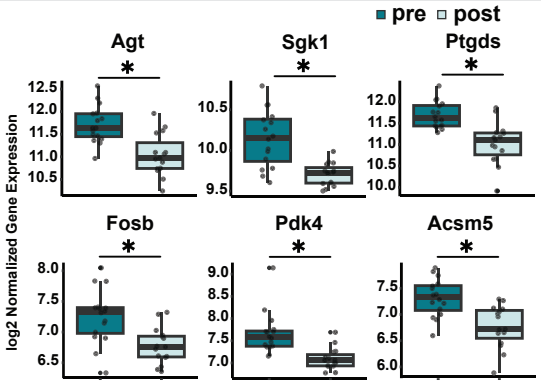

Subgroup analysis of Pre- vs Post-pairing DE genes

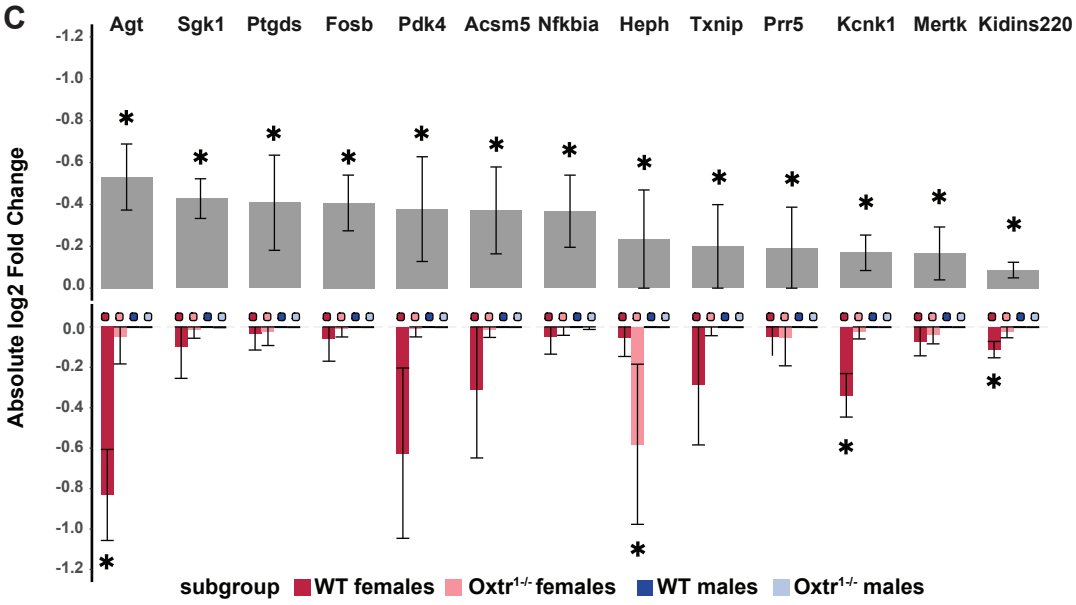

Significant Female Genes

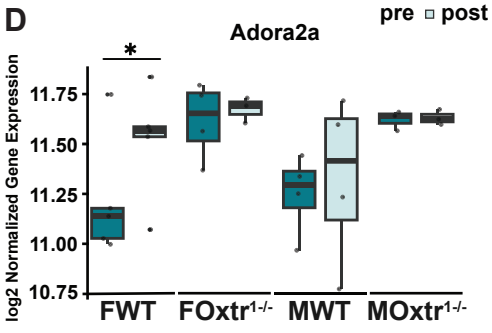

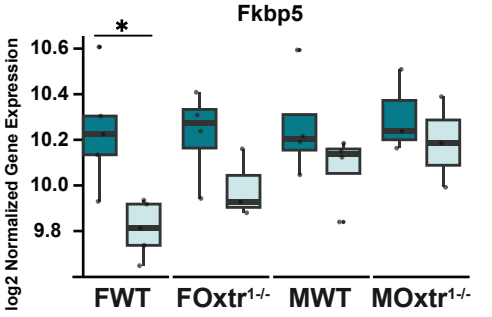

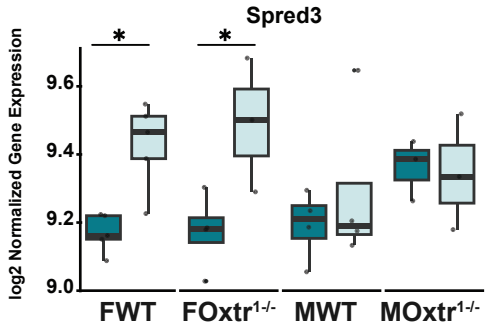

WGCNA: Module correlated with pairing

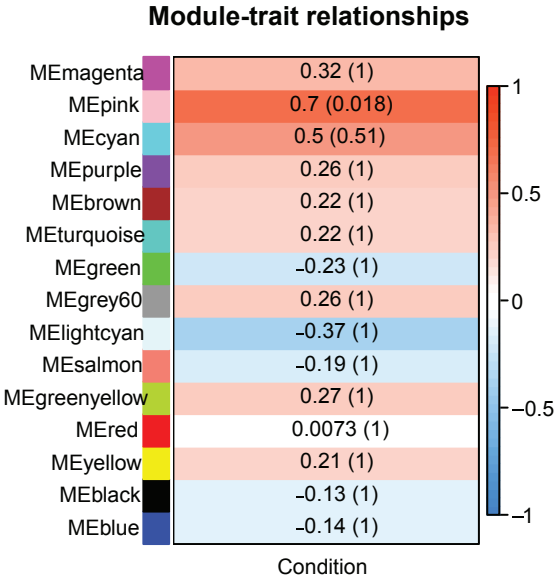

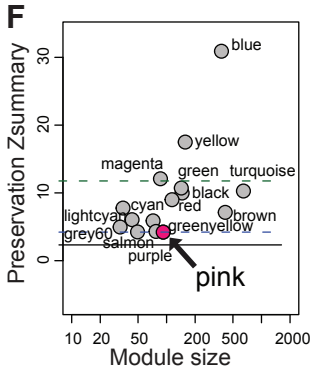

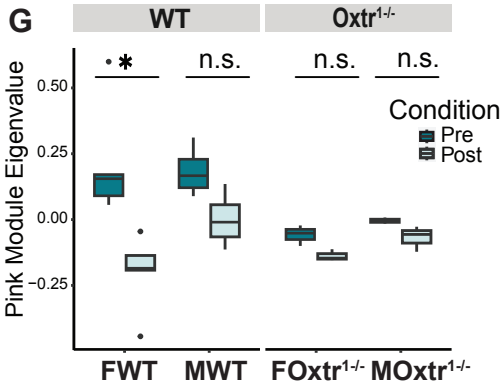

Significant Male Gene

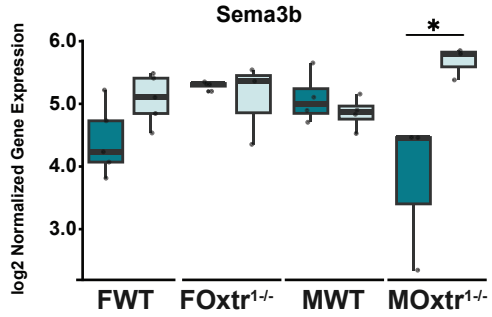

Figure 6: Oxtr regulated genes are common to social behavior relevant processes across species and are similarly regulated across brain regions

Comparison groups for sequencing

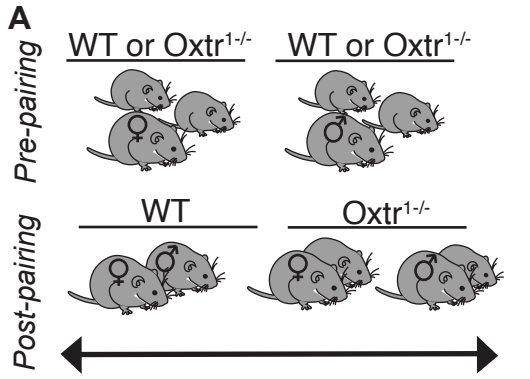

WT vs Oxtr$^{1-/-}$ DE genes

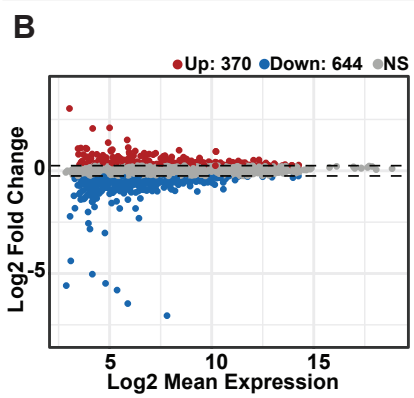

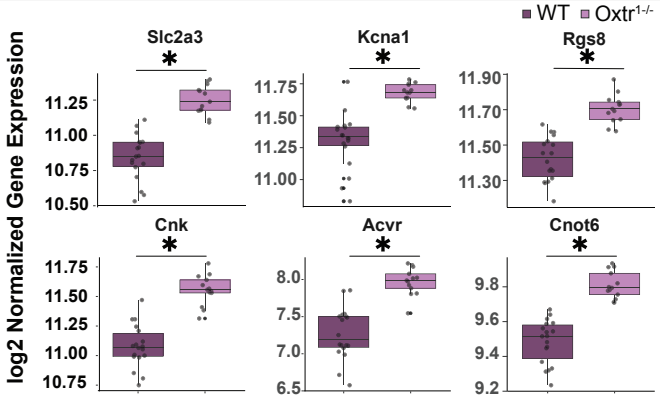

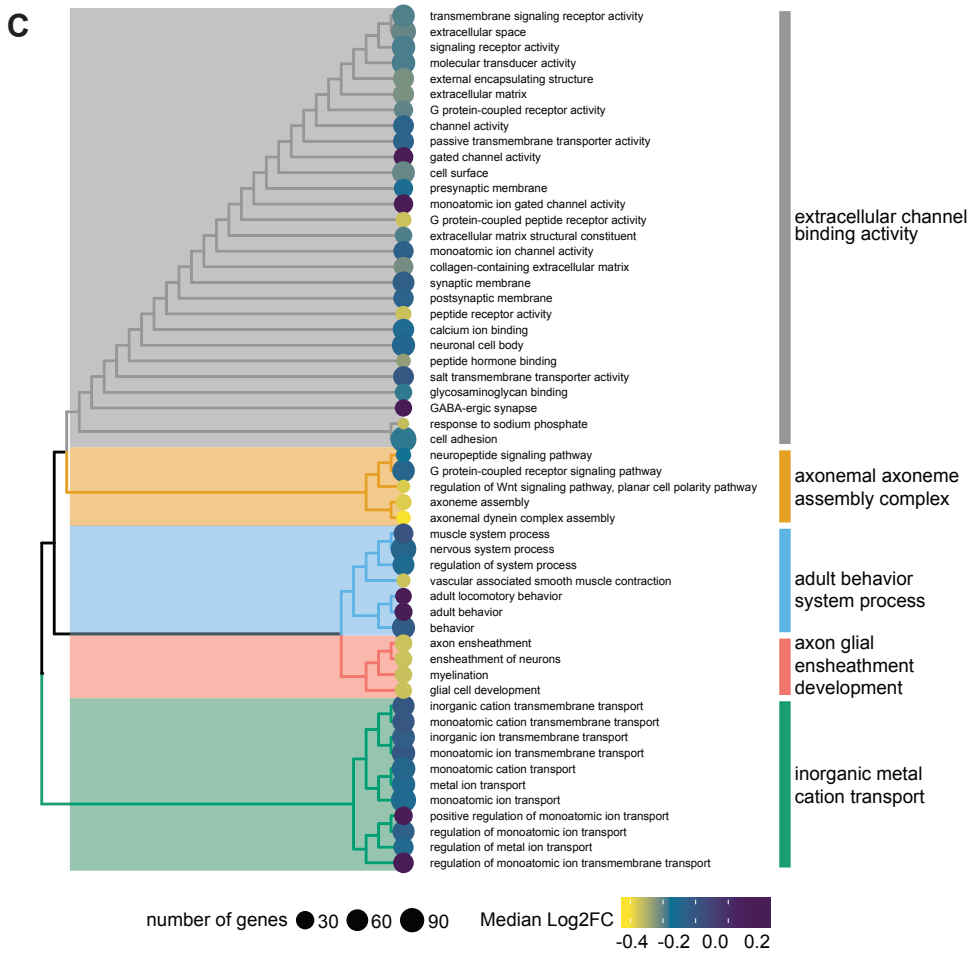

DE gene expression and localization

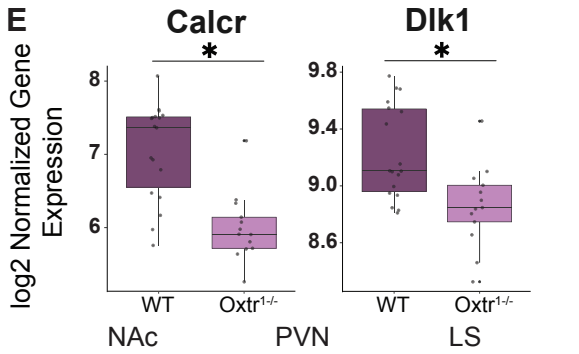

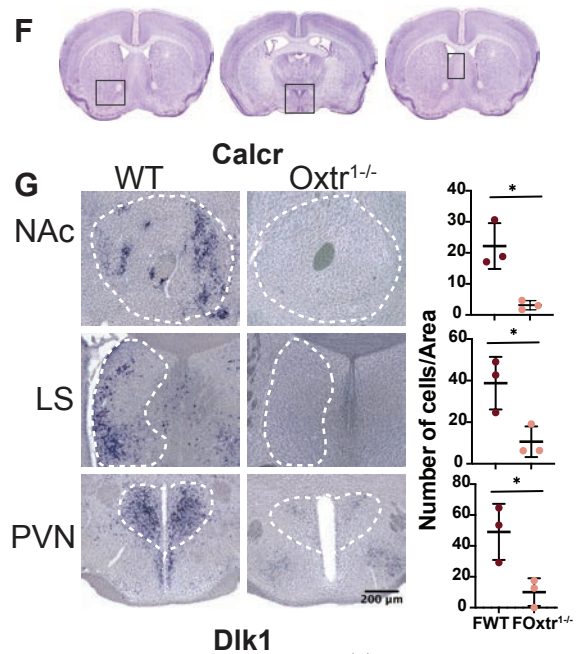

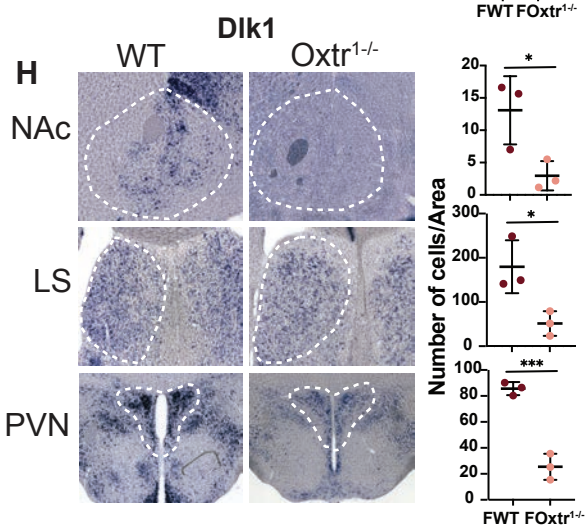

Over-representation of Disease associated genes

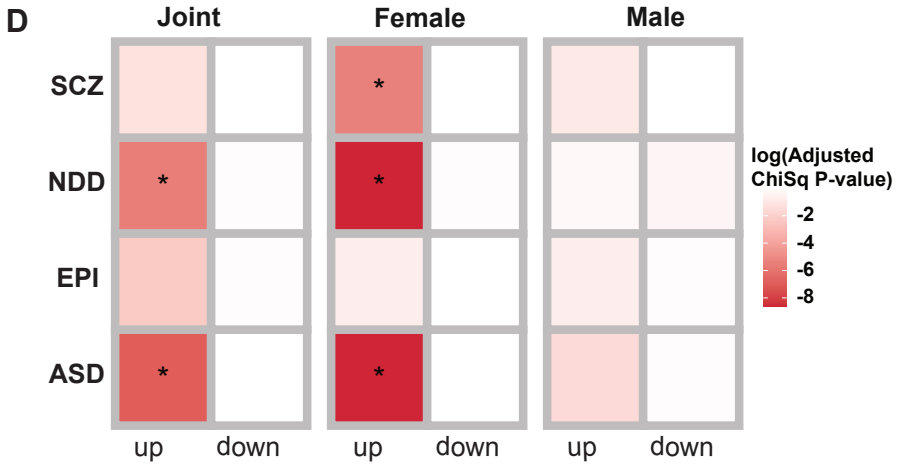
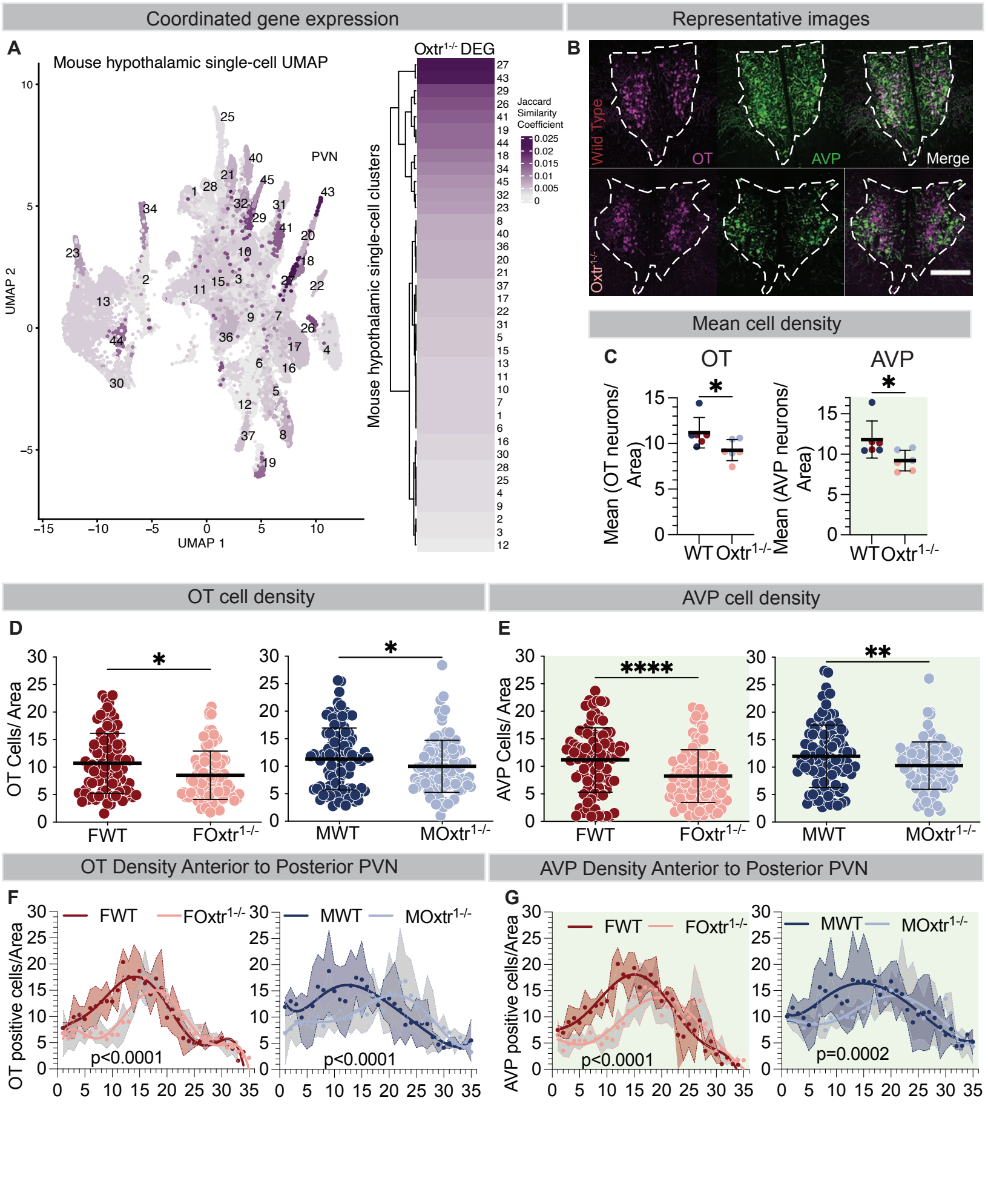
Figure 7: Loss of Oxtr results in the decrease in density of Oxt and Avp expressing neurons in the PVN